

## Chapter 3

# EXPLORATION OF GEOTHERMAL RESOURCES

*Michael Fytikas, Pierre, Ungemach*

Exploration is a significant step in the process of utilization of the geothermal resources. It is aiming at locating geothermal reservoirs for possible exploitation and at selecting the best sites for drilling production wells with the greatest possibly confidence. As with all natural resources exploration, geothermal exploration and development is risky and it is critical that this risk is minimized. Geothermal exploration involves the application of a plethora of methods and techniques from various fields of Earth Sciences (geology, geophysics, geochemistry, drilling technology etc.). Since drilling is very expensive and risky, and taking into account the low heat content of most geothermal fluids, drilling should be considered only as the last research “tool” in order to provide direct data of a prospecting geothermal area. The scope of this chapter is to provide a brief discussion of the main methods in geothermal exploration, from the surface surveys to the drilling of a production well.

Geothermal exploration may be divided into several stages, on a temporal basis:

1. General surface survey
2. Detailed and systematic exploration of most promising geothermal areas
3. Definition of the geothermal fields and study of their characteristics
4. Geothermal field development and management

These stages can be pursued in almost all exploration programmes, but their sequence, the strategy that will be followed and the methods that will be used may differ

from site to site, due to varying nature of the geothermal resources.

### 1) Large Scale Geothermal Survey

The first exploration stage involves the assessment of all the existing geological data and the determination whether favourable geothermal conditions exist in the area of interest. Existing geological and tectonic maps at any scale, aerial or satellite pictures, maps and data from surface thermal manifestations, as well as general geophysical and geochemical maps can be used. All data on thermal manifestations and from warm springs or from existing wells should be evaluated and plotted in a common map. This initial assessment will exclude some areas and may give priority for further exploration to some other areas.

### 2) Detailed and Systematic Exploration of Possible Geothermal Areas

This stage constitutes the most important part of the geothermal exploration, and it is aiming at the determination of the suitable sites for deep drillings. All data and measurements collected for an area (geological, tectonic, volcanological, stratigraphic, lithological, hydrogeological, geochemical, geophysical, thermodynamic, etc.) are carefully examined and evaluated to characterise this area from a geothermal perspective. The target of this stage is to approach the geothermal model of each geothermal reservoir-field and to acquire the knowledge of place and situation in which the geothermal fluids or the hot rocks are located.

The first method applied in this stage is a geological study of the area in order to define the type and the nature of geologic formations, their lithological characteristics and stratigraphy, the thickness of each formation, its permeability etc. It also includes the geological mapping at an appropriate scale (e.g. 1/10000 or 1/20000).

In volcanic areas additional and special volcanological study is required, especially if volcanoes are either active or potentially active. The magma chamber volume is determined through geophysical studies (mainly gravimetry or active seismometry). The chamber depth is determined by the crystallization pressure of its interior, as well as by geo-thermometric and geo-barometric balance methods among the solid phase and the magmatic fluid. The study of hydrothermal alterations of the rocks and of mineral deposits provides important information on the characteristics of the reservoir cap. Furthermore, the nature of the explosive products may allow the determination of the reservoir temperature characteristics through xenoliths.

Understandably, rock permeability plays an important role in a geothermal reservoir. Primary permeability is attributed to the nature of the rock types encountered and to hydraulic characteristics of many favourable geological formations; secondary permeability is attributed to hydrothermal and mainly to tectonic factors. Tectonic factors may indeed influence the geothermal condition of an area, creating faster circulation and ascending of deeper and hotter fluids and resulting in much higher thermal gradient in the area.

The normal faults with extension tectonics create large and open pathways for the circulation and ascending of thermal fluids. As a rule, large normal faults are the main causes for heat transfer towards the surface with hot springs.

Geothermal fluids are in large quantities in rocks (karstic or other cavities), open faults and intermediate pores, even in mineral structure and they usually move quite slowly in the sub-soil on the geological formations within which they circulate. As it is well known, the underground water circulation depends on the hydro-geological

structure of the wider area in it circulates.

Meteoric or surface water descend depends on the type and lithology of the rocks and the tectonic structure. The horizontal underground circulation is certainly influenced from the type of the rocks. The water ascend is facilitated by either normal faults, or by favourable geological structures (e.g. penetrating structures, risen sediments, horsts, anticlines).

The available quantity of geothermal fluids primary depends upon hydrogeological, and secondary upon hydrological and geomorphological conditions. The quantity of ground water circulation in the subsurface depends on the structure of the flow pathways, as well as on physicochemical conditions of geothermal water itself. Hydrothermal alteration of the rocks, in which hot waters circulate, reduces or minimizes the permeability and storage capacity of the formations.

The fault tectonics usually creates large "empty" spaces, where - in combination with mylonitization zone - waters easily circulate. This way, a secondary permeability and storage form for underground waters is created.

The volcano-tectonics and volcanology in general influence the underground hydrogeological circulation and geothermal condition. At best, they create closed or almost closed hydrological basins. Tectonic grabens that were filled with recent and loose sediments are full of meteoric or other surface waters which take over the pores of hydro-permeable formations.

The raising of thermal fluids in older basins occurs during the layering; the existence of hot springs is influenced by intervention of young faults or by natural surface appearance of permeable layers at the sides of synclines.

### **3. Geochemical Methods in Geothermal Exploration**

The geochemical study of geothermal fluids (as well as of solid rocks) is the most widely spread and fairly reliable method for exploration and study of the geothermal areas. The underground circulation of thermal waters and solutions creates certain conditions in which the fluids influence the

rocks, while at the same time they are being enriched in certain elements, gases etc. At a certain point this procedure may be reversed: the mineral content of the fluids is reduced because of the mineral deposition.

The most common phenomenon is the creation of new hydrothermal minerals and the alteration of the original rocks. These phenomena chemically modify the underground hot fluids as well as the geological formations in contact with them. Subsequently, the study of geothermal fluids and hydrothermal influences in surface geological formations, or formations at small depths, is a significant tool for the understanding of the contemporary or recent geothermal situation in the area under exploration.

Geochemical research uses the surface or subsurface fluids from springs, fumaroles, wells and shallow drillings. Sampling and measurement points are selected through various criteria, depending on the exploration stage, the distance of each other, depth, physico-chemical characteristics and the representativeness of each point. Hot fluids are generally preferred, but for comparison samples from cool and warm waters or natural surface reservoirs are collected as well. The bulk of the studied fluids come from hot springs and drillings. This is the reason why representative samples from waters circulating in different formations and reservoirs need to be taken, so that the chances of tracing fluids of deep geothermal origins are significantly improved. Thus, the exploration and chemical analysis of the largest possible number of water samples statistically enables the discovery and study of waters from deeper origin, and mainly of mixtures of surface and geothermal waters.

Within the frame of the usual preliminary study water samples for analyses are taken from wells and drillings of the promising area. Special attention should be given to the origin of these samples, so that they include water coming exclusively from the reservoir, the drilling or the well. Fluid sampling should be repeated in regular hourly or daily intervals, until the analysis produces a stable chemical composition. At this point it is assumed that the fluid represent the reservoir fluid. Reliable sampling techniques

are essential.

## 5. Geophysical Methods in Geothermal Exploration

Geophysical science has developed many methods applied in geological exploration in order to define the main characteristics of the geothermal reservoirs and the regional geology. These methods are selected on case basis depending on the problem in question. It should be noted though that the methods are indirectly; therefore they should be used in combination with other methods (geochemical, tectonic, etc.). The particular geophysical methods applied in geothermal exploration are the follows:

### (a) *Electrical methods*

The electrical methods aim at measuring the electrical resistivity (or its reciprocal, the electrical conductivity) of various rock layers. In general, dry rocks are not good electrical conductors and they exhibit high resistivities, which increases with temperature. For instance, if the resistivity of a rock at 18°C is 100 ohm/m, its resistivity is only 33 ohm/m at 100°C. Low electrical resistivities could be attributed to the existence of underground formations with increased temperature and salinity, i.e. geothermal reservoirs. However, the reverse procedure is not necessarily valid, because many factors influence the resistivities, such as the clay content and the porosity of a rock.

The specific methods used in the geoelectric surveys are:

- 1) galvanic resistivity method,
- 2) iso-potential lines method,
- 3) induced polarization method,
- 4) self potential (or spontaneous polarization) method, and
- 5) telluric currents method.

The galvanic resistivity method and the telluric currents methods are the most common methods in geothermal exploration.

In the galvanic or apparent resistivity method, resistivity measurements are made by passing an electrical current into the ground using a pair of electrodes and measuring the resulting potential gradient within the subsurface with a second (potential) electrode pair (Fig. 3,1). Resistivity surveys involve the gradual increase of the spacing

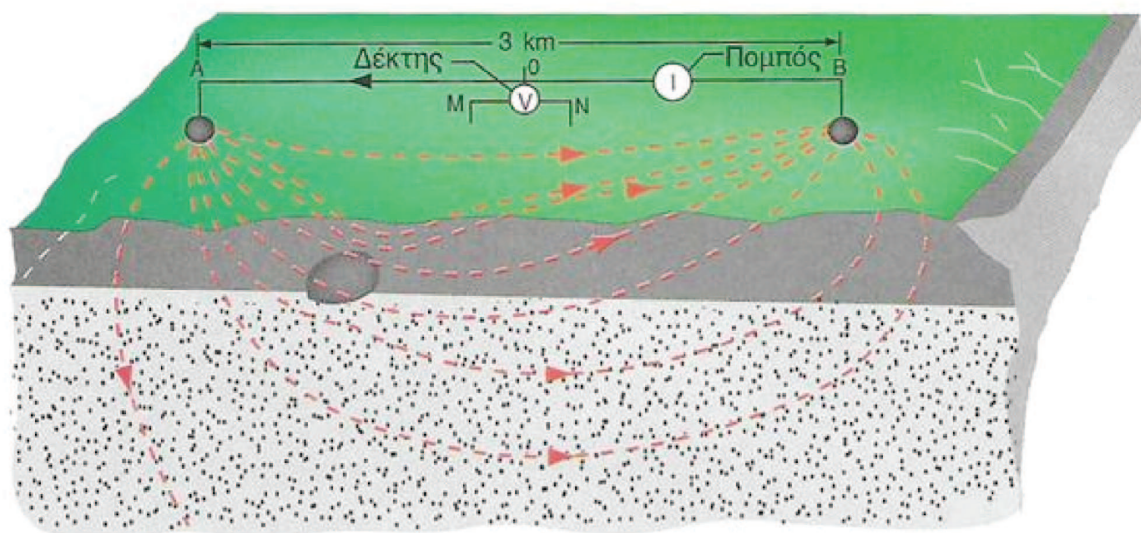


Figure 3.1. Schematic representation of a resistivity survey. Electric current is introduced in earth through the electrodes A and B and the voltage difference between M and N is measured (Barbier, 1997).

between the current/potential electrodes in order to increase the depth of investigation.

The collected resistance data are converted to apparent resistivity readings which can provide information on the thickness of individual resistivity layers within the subsurface. There are several configurations of the electrodes, some of which are shown in Figure 3.2. The commonest arrays are the Schlumberger quadripole and the dipole-dipole array.

The **telluric currents** method is based on electric voltage measurements attributed to telluric currents, which are the natural electrical currents flowing on earth surface, or close to it. The voltage decrease between two points of a telluric current electric line depends on the apparent resistivity of the material located between these two points. The telluric currents method is used increasingly in recent years, since the method enables the study of electrical properties at a larger depths. The method does not produce significant practical results, since it provides information on deep rather than shallow formations.

Another electrical method is the **self-potential** (SP) method, which is a passive electrical technique that involves measurement of naturally occurring ground potentials. Measurements are made using a pair

of non-polarising electrodes connected to a high impedance voltmeter.

**Magnetic** methods are the oldest geophysical sounding methods applied in geothermal explorations. The principle of each geomagnetic method is based on magnetization tracing of the rocks within the earth crust layers. This is achieved with small scale magnetic anomaly measurements on the earth surface, which essential are the geomagnetic field tension changes. The main instruments used are *electronic magnetometers*. The magnetic method involves measurements from both ground areas and from air (air-magnetic measurements).

*Ground magnetic measurements* are successfully and inexpensively applied mainly in areas with hydrothermal alternated zones. *Air magnetic measurements* contribute to the research of geothermal fields and are accomplished with the use of an electronic magnetometer transported on an airplane measuring the total tension of the magnetic field. These measurements enable the tracing of large faults, covered tectonic and other geological structures. These measurements are distinguished in low and high sensitivity measurements interpretation of air magnetic measurements enables the making iso-depth lines maps.

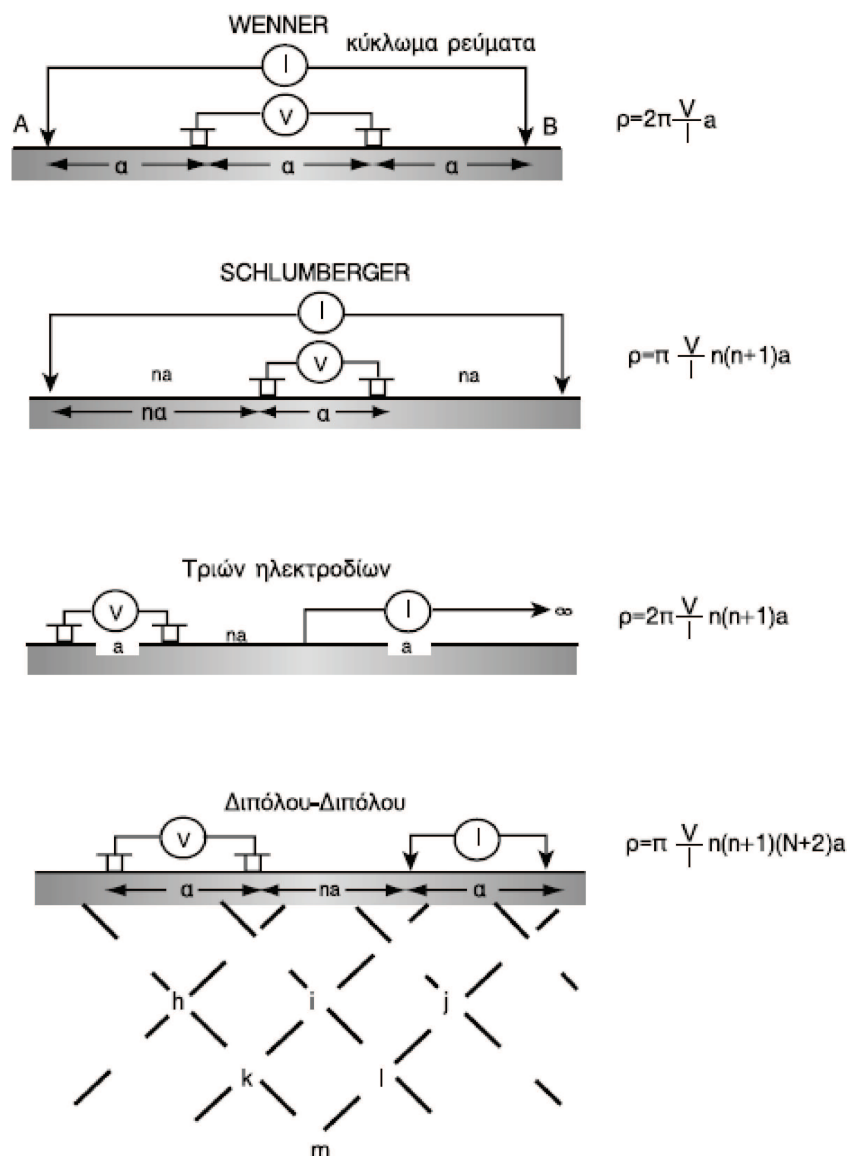


Figure 3.2. Electrode configurations in the galvanic resistivity method.

The main disadvantages are the high cost and the lack of satisfactory accuracy.

The **gravity** method studies the changes of earth's gravity field with tension field measurements (gravity acceleration) in a particular place (Fig. 3.3). Adequate mathematical processing isolates the field components attributed to morphological structures. In addition, the method can possibly create the subsoil structure model in the form of density discontinuations, which – obeying to certain natural and geological restrictions – can satisfactory simulate reality.

The gravity method provides data adequate for tracing various tectonic formations

of the area under exploration, as well as for determining their characteristics. Furthermore, it has been observed that certain “self-sealing” former reservoirs are associated with gravity anomalies.

The most important factors that influence the measurements taken with gravity method are the tension dependence on the geographical latitude, altitude, rock mass in between two points (Bouguer result), area topography, the instrument itself, and earth tides. Bouguer anomaly ( $\delta g$ ) can be calculated and is used to determine the gravity structure. The most common terms for peripheral caused anomalies are peripheral

anomaly Bouguer, general field, or general anomaly. This distinction is imperative, because the gravity research's target is the isolation of the structure results concerning the particular research.

The gravity method is used extensively in geothermal exploration and combined with other geophysical methods or geological observations that provide important information on the distribution of the "anomalous" mass.

The tectonic characteristics of the base – as revealed through the interpretation of Bouguer anomaly – are particularly important for the study of a geothermal field, since their awareness enables the potential understanding of the geothermal fluid circulation and the whole thermal situation.

The basic individual **seismic** sounding methods are the seismic **reflection** method and the seismic **refraction** method. In addition and within the framework of the seismic method, some other methods spawn satisfactory results. These are the **automatic polarization** method, the **micro-seismic** sounding and the study of **seismic noise**.

The seismic sounding method aims at determining the diffusion speed change of the elastic (seismic) waves within the surface earth crust layers. This is achieved through measurements of these waves' trail timing within these layers and through application of known Physics laws that determine this diffusion. After diffusing in the surface layers of the earth crust, these waves are reflected through various surfaces (seismic reflection) and return to be recorded by sensitive seismometers called *geophones* in various distances (Fig. 3.3)

Based on the elastic waves' records the distance timing curves are created; these curves are used to calculate the diffusing speed of the elastic waves in connection to the depth. The knowledge of the speed change within the surface layers of the crust can possibly lead to the tracing of tectonic structures with geothermal interest. An example of the above situation is the tracing of faults, in which geothermal fluids circulate, the specification of tectonic horsts, which are highly favourable for the creation geothermal reservoirs, etc.

The seismic method includes the **ref-**

**raction** of the waves within the formations. The manner of the waves' course - which is different among formations – is determined along with discontinuations (faults or side alternation of geological formations).

The seismic sounding method is a particular important method in geothermal research and it has been used in many occasions in order to study the tectonic structure and geothermal potential of an area. The seismic methods and particularly the seismic sounding have high cost in comparison to other geophysical methods.

Seismic reflection method is the most commonly used and it is a very important fact for geothermal research, since it enables the tracing and mapping of geothermal reservoirs. The seismic reflection method is hard to apply to areas with large volcanic structures and particular to areas with frequent side alternations due to multiple volcanic centers. When the geothermal field's reservoir is located under clayely conductive layers, its mapping with the use of geoelectric methods is impossible; in this case seismic methods are used.

Seismic refraction method is useful in morphologically anomalous areas, where other methods are unsuitable. However, it is less accurate in comparison to the reflection method; it also presents difficulties during measurements because the used geophones are distributed in long distances.

**Automatic polarization** method can provide valuable information for geothermal fluid circulation located in small depths; it is also characterized by low application cost. It is used in geothermal field cases where the reservoir's self water-tightness and the faults' and fractures' re-activation is a frequent phenomenon of primary geothermal importance.

In seismic areas in particular, seismic activity creates new faults and fractures, which allow the circulation of geothermal fluids. Consequently, the study of *active seismic activity* – even of small vibrations – is an essential geothermal research element. In most geothermal fields, micro-seismic activity and high level ground seismic noise is observed. *Micro-seismic study* and *ground noise study* is an almost cost-free large-scale study and interpretation method for

geothermal fields. It can be done with the installation of a network of seismographs in both the area in question as well as in the general area, for a detailed record of the seismic activity. This procedure determines

the active faults, the zones of differentiation in the transference of waves due to the circulation or the entrapment of geothermal fluids, etc.



## Chapter 4

# WELL, RESERVOIR AND PRODUCTION ENGINEERING

Pierre Ungemach

### 4.1 INTRODUCTION

From exploration to production, from expectations to achievements this is what this chapter is all about. It follows the phases, streams and interactions sketched in fig. 4.1.1.

Once surface and subsurface exploration is terminated, direct assessment of the candidate reservoir (s), via drilling, comes into play.

The next step consists of testing the wells, while drilling and after completion, together with multiwell tracer tests. Added to lithologic, structural and fluid sampling information gained during drilling/testing, they provide a data base for (i) an evaluation of well performances, (ii) a preliminary assessment of the reservoir(s), and (iii) last but not least, implementing, after integration of previously acquired surface/subsurface reconnaissance shows and findings, the so-called conceptual model, indeed a crucial step, setting the base for further reservoir simulation and assessment stages. Simulation is a three stage process, from natural state modelling and validation of the conceptual model to, history matching, model calibration and predictive modelling of future production scenarios.

Heat extraction contemplates three production issues, *power generation* (flash cycles), *combined heat and power* (CHP) using *binary cycles* (ORC) and *direct*

*uses/shallow heat pumps* according to high, medium and low source fluid enthalpies respectively. *Enhanced geothermal systems* (EGS), the new geothermal frontier, may fit in the extraction process, most likely through CHP systems. Ultimately, reservoir management will ambition optimising heat extraction by sustaining production and reservoir longevity via water injection and make up wells.

Material balance is mentioned for its simplified approach to reserve estimates and long practiced lump parameter modelling.

Special emphasis has been placed on well testing and reservoir simulation/numerical modelling, as a credit paid to methods, which are the core of quantified geothermal reservoir evaluation.

### 4.2 DRILLING AND COMPLETION

Geothermal drilling covers a wide spectrum of objectives, ranging from shallow to deep, from slim to large diameters, from exploration to development targets, from sedimentary to hard volcanic/crystalline rock environments.

However, there are no specifically designed geothermal drilling rigs and equipment. Hence, the standard petroleum and ground water and, exceptionally, mining drilling technologies applies to geothermal exploration and production.



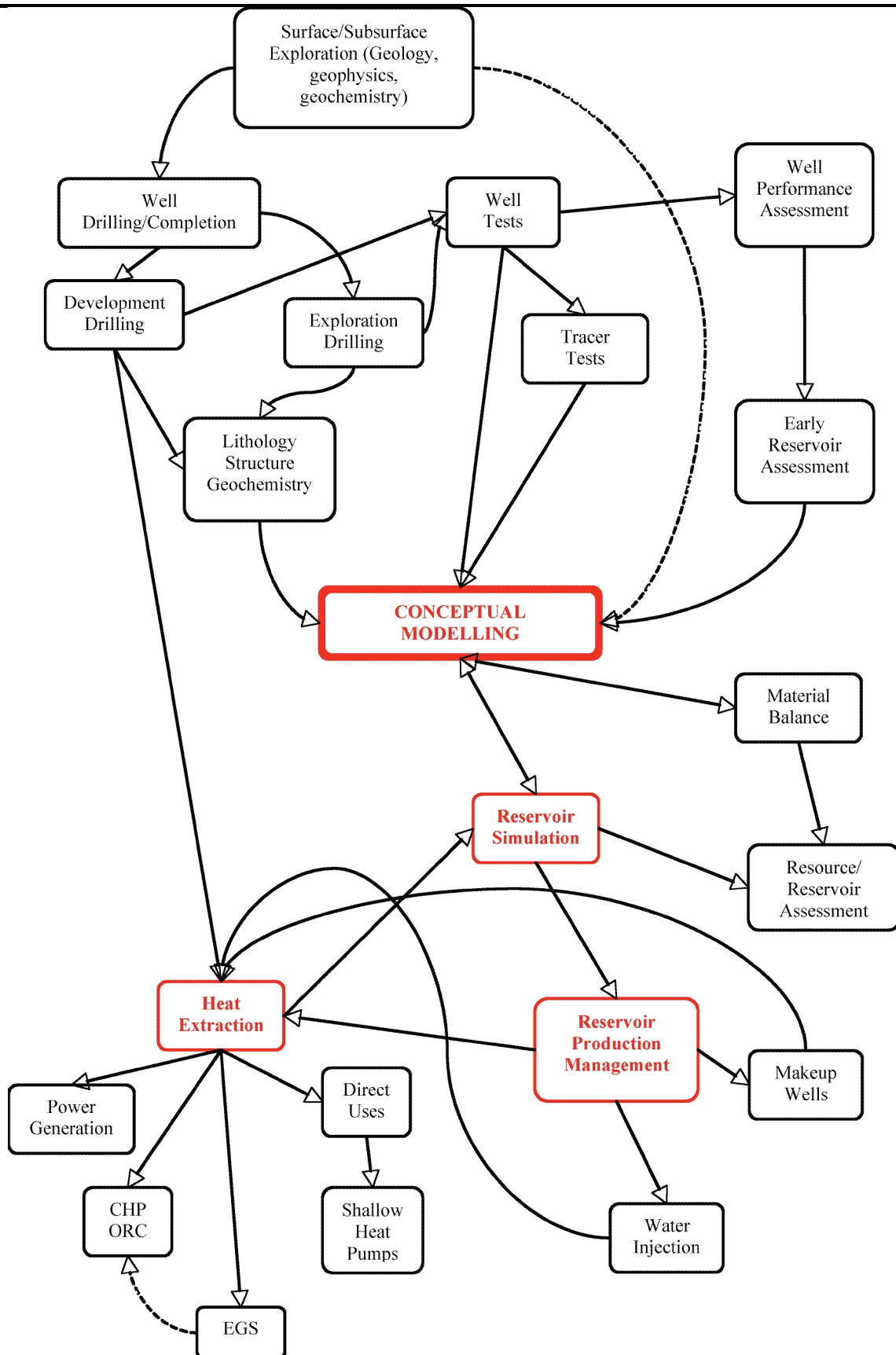
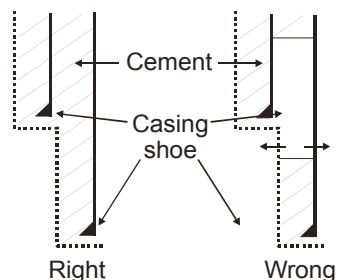


Fig. 4.1.1 – From Surface Reconnaissance to Reservoir Management

Only formation lithology and temperature, and extensively fractured reservoirs, require special attention while tackling high enthalpy settings. Well site geology, for instance, would demand more petrography/volcanology oriented skills than the casual sedimentary calcimetry monitoring inherent to, sedimentary, hydrocarbon drilling. Drilling fluids need to be cooled via an areofrigerant tower. In order to accommodate thermally induced expansion/contraction, well heads should be equipped with expansion spools. While intersecting reservoir fractures, severe lost circulation occurs, which require underbalanced foam drilling procedures. Otherwise, rock hardness and texture is more a matter of tool (bit) to rock adequacy than a drilling problem proper. Completion of geothermal wells is generally simpler than in the petroleum and groundwater sectors. Slotted or perforated liners prevail in high enthalpy completions and openhole and, more seldomly, screen/gravel pack assemblies in direct use wells.



With respect to cementing, every casing phase needs to be cemented above the previous casing shoe (see attached sketch) to avoid undue boiling of trapped fluids and subsequent casing collapse caused by thermally induced shear. At exploration stage, shallow reconnaissance wells are drilled for lithostratigraphy control, geochemical sampling and heat flow measurement purposes, thus providing clues for locating deeper drilling targets within the larger area delineated thanks to previous geological, geophysical and geochemical investigations.

The profile of such shallow drill holes stands usually as follows.

- 0-150/200 m: cased hole 7".
- 150/200-150/250 m: open hole 6" or slotted liner 4" 1/2.

The microdrill mining technology allows

to drill safely medium depth reconnaissance slimholes, until ca 1000 m depths, and provide coring, logging and sampling and, occasionally, testing services routinely operated by the mining industry.

Ultimately, deep, large diameter, exploration, step-out and development drilling will become the rule.

A typical exploration well would match the following profile.

- 0-50 m: conductor pipe 24".
- 0-300 m: 18"5/8 casing.
- 0-800 m: 13"3/8 casing.
- 750-1600 m: 9"5/8 liner.
- 1550-2000 m: 7" slotted (perforated) liner.

The completion of an optimised development well could conform to the following design (drilling deviated wells).

- 0-50 m: conductor pipe 24".
- 0-400 m: 18"5/8 casing.
- 0-900 m: 13"3/8 casing.
- 450 m: deviation kick off (KOP).
- 450-800 m: deviated trajectory build up (mud motor/steering).
- 850-1750 m: 9"5/8 liner.
- 800-2300 m: deviation drilling (rotary assembly).
- 1700-2300 m: 7" slotted (perforated) liner.

Slotted (perforated) liners have basically a propping rather than (particle) filtering function. In low enthalpy, direct use, well design, open hole completion prevails in consolidated carbonate environments.

Drilling fluids avoid nowadays environmentally sensitive compounds, such as lignosulfonates including heavy metals. Geothermal drilling fluids include bentonite, lightweight suspended solid additives (puzzolane, attapulgit), biodegradable polymer formulae, water, air, aerated water and foam.

Bits are of the tricone roller bit and polycrystalline diamond (PDC) types.

Otherwise, geothermal deep drilling works benefit from recent technological breakthrough in the areas of drillstring drive, monitoring, deviation drilling and rock bits. Nowadays, top drive, high torque, power swivels are substituted for conventional floor kelly drive, measurements while drilling (MWD) inertial/gyroscope (instead of previous single/multishot compass), surveys, performant downhole mud motors and po-

lycrystalline diamond bits have definitely taken the lead.

High entahlpy, geopower targeted, and, direct use, low enthalpy drill sites address contrasted environments, remote/quasi desertic against densely populated respectively.

The latter must comply with stringent environmental regulations, with respect to noise and waste disposal, requiring electric rig drive and efficient waste processing/abatement procedures.

Drilling represents the major cost segment in any geothermal undertaking whatsoever. From 2004 to 2006, well drilling/completion costs have increased by 30%, trending, as of 2006, at ca 3.5 million euros for a 2500 m deep well. Therefore, optimum well design and drilling programmes/schedules are needed to meet project feasibility requirements.

The available, and most commonly used, geothermal drilling techniques are summarised in fig. 4.2.1.



Fig. 4.2.2 – Geothermal drilling method (source: Thorhallsson, 2007)



Fig. 4.2.3 – Geothermal drilling. Melun. France (source: GPC/Sedco-Forex)

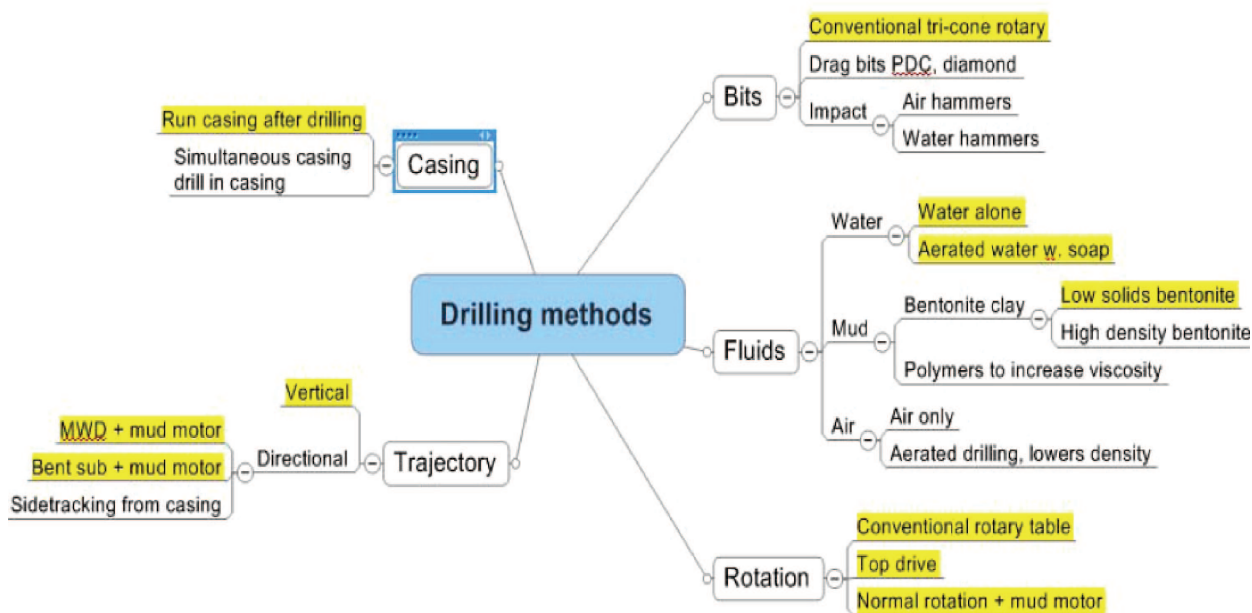
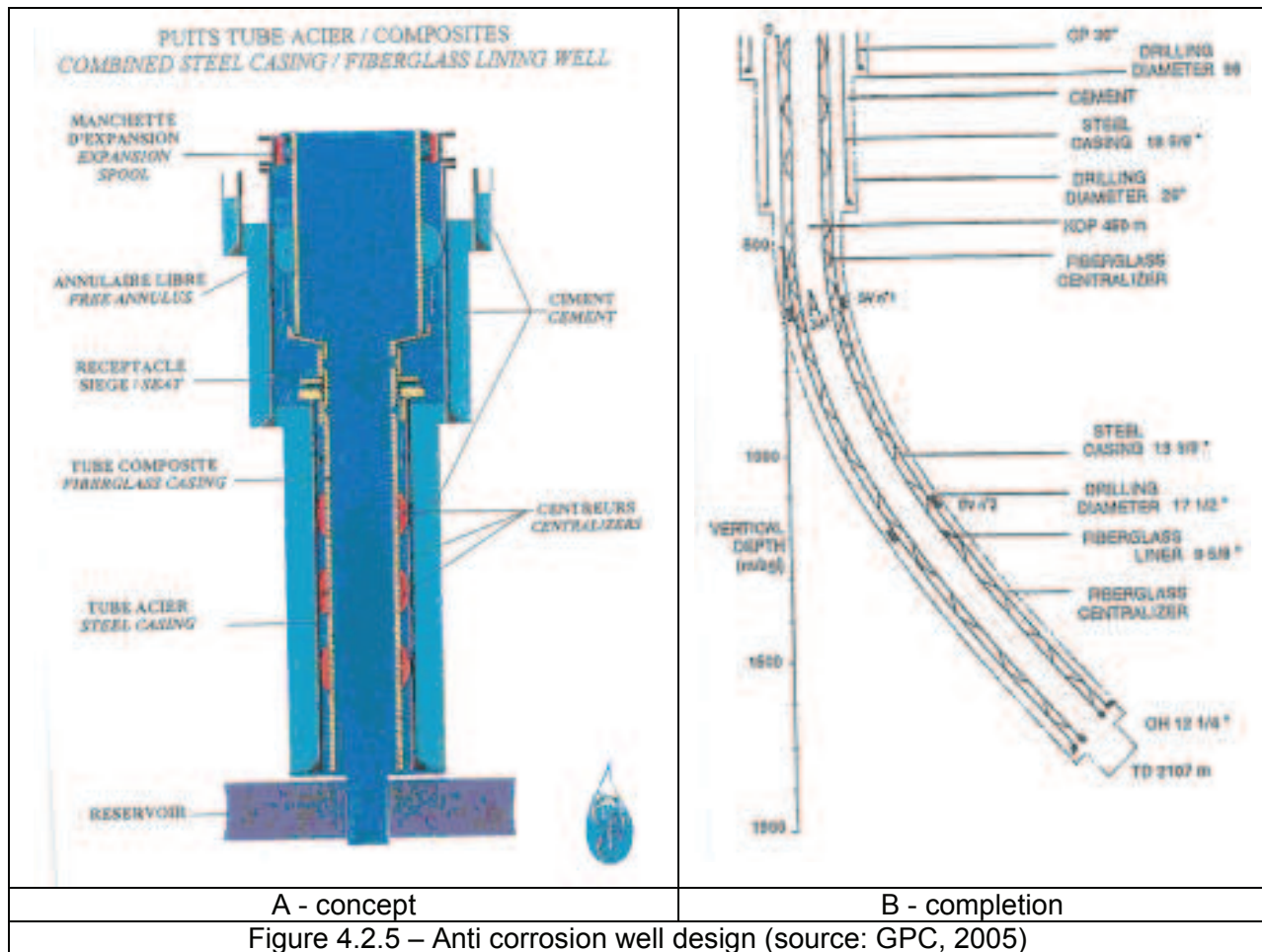


Figure 4.2.4 – Geothermal drilling method (source: Thorhallsson, 2007)

Cutting down rig time costs is a prerequisite. Fig. 4.2.2, limited to the mud motor vs conventional rotary drilling alternative defends and illustrates this rationale, leading to an almost 50% gain in rig time. Underbalance drilling and PCD bits shape equally as candidates to upgrading drilling performance.

Figures 4.2.4 to 4.2.7 exemplify various well drilling/completion strategies and achievements. Fig. 4.2.6 depicts the anti corrosion well concept, completed in 1995 on a Paris Basin geothermal district heating doublet, combining steel propping casings and fiberglass production liners with a free annulus.



Well completion, based on a 35° deviated, 2100 m, 17”1/2 diameter deep trajectory required the mobilisation of a 350 t, diesel electric, rig.

Fig. 4.2.5 illustrates the case of a 350 m deep well, drilled in a hot, fresh water, karstic environment, in the Southern Germany (Bavaria) Molasse Basin. Here, the well was drilled vertical until it reached the presumed top reservoir depth, leading to a ca 40° deviated trajectory, aimed at intersecting subvertical reservoir fractures, shaping orthogonal to the main local normal fault.

Completion design of an injection well,

drilled in clastic sedimentary deposits sensitive to particle induced plugging, is shown in fig. 4.2.7. Here, the target injection rate at sandface, velocity and particle filtering cut were set at 150 m<sup>3</sup>/h, ca 0.3 cm/s and 5 μm respectively in order to secure the waste water injection issue.

Fig. 4.2.8 is an illustration of a water/ water heat pump heating/cooling doublet based on a dual aquifer completion scheme in a sandy formation context, casual in petroleum production but unusual in geothermal/groundwater projects.

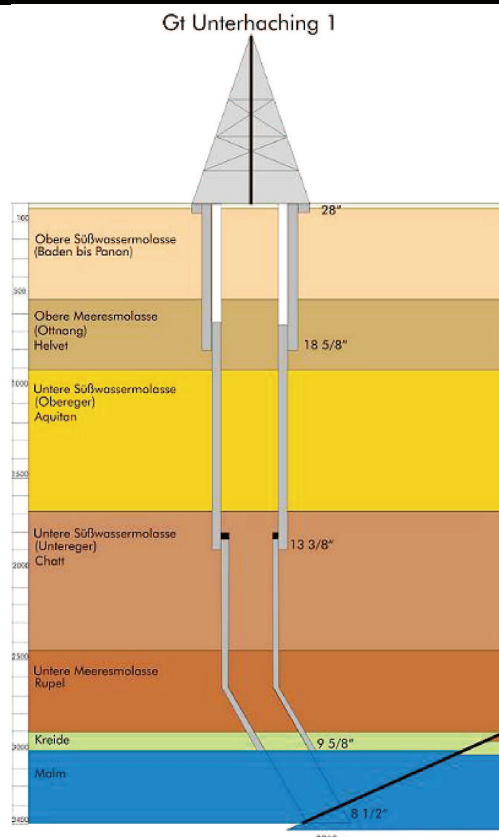


Fig. 4.2.6 – Unterhaching 1. Well completion (source: GTN, 2006)

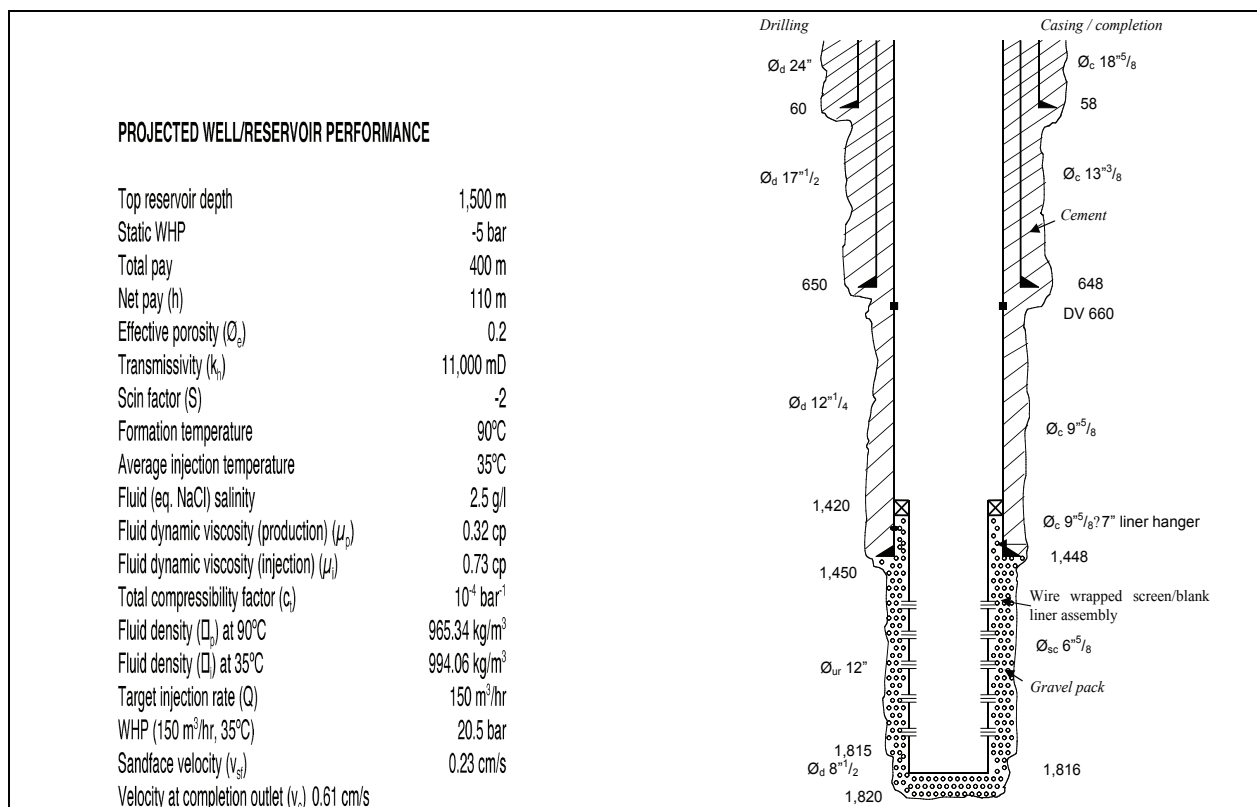


Fig. 4.2.6: Injection well completion design. Sandstone environment (GPC, 2003)

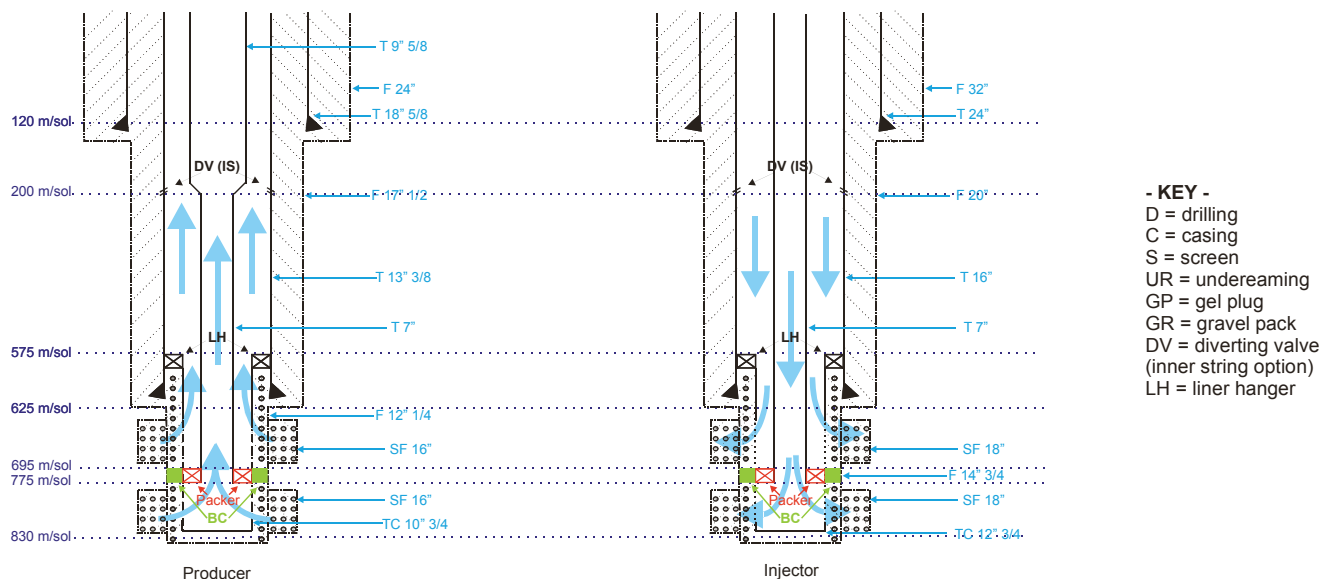


Figure 4.2.7 – Dual, heat pump oriented, water well completions. Note that the producer well can be equipped with two submersible pump sets (source: GPC IP, 2007)

### 4.3 WELL LOGGING/TESTING/TRACING

#### 4.3.1 Well logging

Geothermal well logging deals with three major concerns (i) reservoir exploration, (ii) reservoir development, and (iii) resource exploitation / management respectively.

- Hence logging requirements address the following headings.
- Geological framework : lithostratigraphic control, structural features
- Reservoir characterisation : geometry, location of productive layers (pay zones), hydrothermal convection, pressure/temperature/flow patterns
- Fluid properties
- Design and control of well casing/completion
- Monitoring of well integrity during exploitation

These key issues intervene downstream from former geological, hydrogeological and geophysical (mainly seismic surveys) investigations and speculations.

With respect to low enthalpy geothermal deposits, whose development is fairly recent, their reconnaissance often benefited from previous hydrocarbon drilling campaigns which provided significant well control and data bases. Such was the case of the central part of the Paris Basin. Here, data collected by oil operators, and made accessible to the Public thanks to the

French mining law, were reprocessed and complemented by heat flow measurements leading to a reliable evaluation of the resource base and related resource / reserve assessments. A similar situation was encountered in Central/Eastern Europe particularly in Hungary.

Worth adding is that logging information is (i) limited to the well and its immediate surroundings, and (ii) affected by the noise induced by the drilling fluids and mud cake.

Well logging (and testing alike) has, in the recent years, gained increased reliability from tool technology, data acquisition and, interactive computer assisted, processing software rendering interpretation a truly rewarding exercise.

Logging tools fall usually into three categories, openhole, cased hole and production respectively. To simplify:

- Openhole tools are exploration oriented and deal with formation and reservoir evaluation.
- Cased hole tools aim at well (casing/cement/completion) integrity control.
- Production tools are measuring and sampling devices assisting well tests and fluid analyses.

Exploration tools deserve a special comment. As far as lithostratigraphy, porosity and permeability are concerned there

is no direct in situ assessment of these petrographic and physical parameters. Instead those are measured indirectly through other, physically related, parameters such as spontaneous potentials, resistivities, bulk densities, transit times, natural radioactivity and rock hydrogen contents.

- Other, structural and tectonic features can be appraised via magnetic, seismo-acoustic measurements and image processing applied to dips and fracture determination among others.
- Drilling / completion fluids, mud cake and invaded zone effects, need to be cor-

rected in order to release true (clean) formation figures.

- Tool to tool cross correlations (cross-plots) are currently practiced to improve lithological identification and porosity appraisals.
- The basic formulae, borrowed from Schlumberger (1986, 1987), listed in Table 4.3.1 form the driving rationale of quantitative log interpretation.
- Logging programmes addressing exploratory and development wells are attached in Tables 4.3.2 and 4.3.4.

TABLE 4.3.1 - BASIC FORMULAE USED IN LOG INTERPRETATION  
(after Schlumberger)

$$(1) SP = -K \log(R_{mf} / R_w)$$

$$(2) F = R_o / R_w = a / \Phi^2$$

$$(2') a = 1$$

$$(2'') a = 0.81$$

$$(3) S_w = (R_o / R_t)^{1/2}$$

$$(4) S_w / S_{xo} = \left( \frac{R_{xo} / R_t}{R_{mf} / R_w} \right)^{1/2}$$

$$(5) t_s = \Phi t_f - (1 - \Phi) t_{ma}$$

$$(6) \Phi = (T_s - T_{ma}) / (T_f - T_{ma})$$

$$(6') \Phi = 0.67 (T_s - T_{ma}) / T$$

$$(7) p_b = \Phi p_f - (1 - \Phi) p_{ma}$$

$$(8) \Phi = (p_{ma} - p_b) / (p_{ma} - p_f)$$

*Archie*  
*Humble*

*Wyllie*  
*Raymer-Hunt-Gardner*

#### Parameters

F	= formation factor
K	= SP (temperature dependant) constant
R	= resistivity
S	= saturation index
SP	= Spontaneous (self) potential
T	= transit time
$\rho$	= density
$\square$	= porosity

#### Subscripts

b	= bulk rock
f	= fluid
ma	= matrix
mc	= mud cake
mf	= mud filtrate
o	= (clear water saturated formation)
t	= clean formation
s	= sonic
w	= water
xo	= flushed zone

TABLE 4.3.2 - BASIC LOGGING TOOL NOMENCLATURE

LOG NAME	ABBRE- VATION	WELL STATUS	APPLICATION
Gamma Ray	GR	OH, CH	Argillosity Lithology marker
Spontaneous (Self) potential	SP	OH	Lithology, porous/pervious layer marker
Dual Induction	DIL	OH	Lithology, formation resistivity
Dual Laterolog	DLL	OH	Lithology, formation resistivity
Litho Density	LDL	OH	Lithology, density, porosity Porosity/lithology crossplots
Compensated neutron	CNL	OH, CH	Porosity. Porosity/lithology crossplots
Borehole Compensated Sonic	BHC	OH	Porosity. Porosity/lithology crossplots
Formation Micro Scanner	FMC	OH	Extension of the dipmeter tool (SHDT). Formation imagery. Fracture processing
Borehole Geometry, Caliper	BGL, CAL	OH	OH diameter, annular cement volumes
Cement Bond, Variable Density	CBL/VDL	CH	Cementing control
Ultrasonic Inspection	USIT	CH	Cementing control Inside casing inspection
High Resolution Thermometry	HRT	OH, CH	Dynamic/static temperature profile
Quartz Pressure Gauge	QPG	OH, CH	Dynamic/static pressure profile
Production Logging	PLT, PCT	OH	Combined (pressure, temperature, flow) tool.
Full Bore Spinner Flowmeter		CH	Low speed well flowmetering (petal device)
Continuous Flowmeter		OH, CH	Flow profile
Tubing Geometry Sonde	TGS	CH	Casing ID, 16 arm, simultaneously recorded deflections
Multifinger Casing Caliper	MFCL	CH	40 to 60 arm tool Max/Min casing ID
Casing Inspection Caliper	CIC	CH	40 to 60 arm tool Max/Min casing ID
Fluid Sampler	FS	OH, CH	Bottom hole sampling (PVT analysis)

CH = Cased hole  
OH = Open hole



TABLE 4.3.3 - EXPLORATORY WELL LOGGING PROGRAMME

TOOL	DEPTH INTERVAL m	WELL/LOG STATUS	REMARKS
BGL	0 – 2680	OH	Cement volume
BGL/GR		OH	OH flow section
DIL/SP/GR	0-1370	OH	Upper clastics Lithology, porosity
DLL/GR	1375 – 2680	OH	Lower carbonate lithology
BHC/GR	1375 – 2680	OH	Porosity
FMS/GR	1790 – 2680	OH	Reservoir fracturing
LDL/CNL/GR	1375 – 2680	OH	Neutron/density porosities
HRT	0 – 2680	OH/CH	Static/dynamic temperature profile
QPG	0 – 2680	OH/PRO	Static/dynamic profile
PLT	1375 – 2680	OH/PRO	Full bore tool
QPG	2500	OH/PRO	Pressure buildup
BHS	2600	OH/PRO	PVT
GR/CCL	1790 - 2680	OH/CH	

OH Openhole

CH Cased hole

PRO Production logging

TABLE 4.3.4 - DEVELOPMENT WELL LOGGING PROGRAMME

TOOL	DEPTH INTERVAL (m)	WELL/LOG STATUS	REMARKS
BGL/GR	359 – 1905	OH	Cement volume
CBL/VDL/GR	338 – 1880	CH	Cement control
LDR/GR	1907 – 2109	OH	Reservoir only. Lithology / porosity
BGT/BHC/GR	1907 – 2109	OH	Reservoir only. Porosity and diameter
MFCT	+2 – 1895	CH	Inside casing status
USIT	10 – 1906	CH	Corrosion / cement control
PLT	1907 – 2083	OH/PRO	Producing intervals
QPG	1911	OH/PRO	Pressure draw down / build up
BHS	2060	OH/PRO	PVT

#### 4.3.2 Well tests

Contrary to logging, well testing exhibits an investigation power extending far beyond the well face, alongside a regularising (averaging) effect, smoothing the

impact of local heterogeneities. It appears therefore as a relevant tool for quantifying bulk reservoir behaviour.

This stated, well testing is assigned two objectives, namely (i) evaluation of well and

reservoir performance, and (ii) reservoir management.

From testing are derived well deliverabilities which depend on reservoir net thickness, permeability, skin, wellbore storage, static (initial) reservoir pressure, boundary conditions and field singularities, the identified drainage model (matrix or fracture dominated, dual porosity system) and fluid enthalpies, composition and rheology.

Not overlooking well monitoring during production (and injection), reservoir management is closely linked to reservoir simulation which fits single well test data and production/injection histories into a generic conceptual model to forecast future pressure/temperature patterns, temperature breakthrough times, and predict reservoir life.

*Preliminary remarks:*

- Well performance, in terms of well flow and fluid enthalpy, can be estimated at well head by the Russel-James semi-empirical lip pressure expressed as follows (James, 1962)

$$G = 1839 P_c^{0.96} / h_0^{1.02} \quad (4.3.1)$$

Where:

- G = flow (ton/m<sup>2</sup>s)
- P<sub>c</sub> = lip pressure (bar)
- h<sub>0</sub> = fluid enthalpy (kJ/kg)

Eq. (4.3.1) stands valid for low non-condensable gas contents and dissolved solids.

Grant *et al* (1982) proposed a modified gas correction. The limitations of the method can be offset by the use of a separation/metering facility enabling to operate the test at varying thermodynamic conditions.

- Surprisingly, in spite of the complexity and heterogeneous structure of most, especially high enthalpy, reservoirs, pressure transients often reflect the response of an homogeneous reservoir, whereas tracer tests or flowmeter logs would identify a contrasted multilayered structure instead (Ramey, 1988).
- Multiwell, interference, tests are most welcome since they extend the possibilities of single well tests to reservoir porosity and anisotropy determination. They represent also an unvaluable benchmark for further conceptual model validation and numerical mo-

del calibration phases.

*Well test principles*

Non steady state well testing is based on the analysis of pressure transients which, in the ideal case of a single well, discharging at a constant rate (q), a single phase horizontal flow in a homogeneous, isotropic, non compressible porous medium of constant thickness (h) and infinite radial extent is expressed (gravity and thermal effects neglected) by the equation:

$$p_i - p = \frac{q\mu}{2\pi kh} [-Ei(u)] \quad (4.3.2)$$

known also as the line source solution with : Ei(u) = exponential integral function  
 $u = \phi\mu c_t r^2 / 4 kt$

For small values of u ( $u < 10^{-2}$ ) (4.3.2) reduces to the semi logarithmic approximation :

$$p_i - p = 0.183 \frac{q\mu}{kh} \left[ \log \left( \frac{kt}{\phi\mu c_t r^2} \right) + 0.351 \right] \quad (4.3.3)$$

Definitions, symbols and units used are listed in table 4.3.5.

Solution (4.3.2) is exploited by superposition of the bottomhole pressures vs time log-log plot to the -Ei(-u) type curve (identification or match-point method)

Solution (4.3.3) enables to derive the straight line slope (m) of the semi-log plot of pressures vs times (semi-log analysis).

**Well test interpretation**

Whenever an observation well, at a distance r of the producing well (case of an interference test), is not available, pressures are monitored and processed on the sole producing well and r will be set equal to well radius r<sub>w</sub> in compliance with the line source approximation adopted in the sandface flow boundary condition

$$\left( \lim_{r \rightarrow 0} \left( \frac{\partial p}{\partial r} \right) = \frac{q\mu}{2Mkh} \right).$$

in the forthcoming p □ will be referred to as the well flowing pressure p<sub>wf</sub> (see Table 4.3.5).

- *Log-log plot. Type curve/match point analysis*

The reservoir is assumed of infinite radial extent and the well subjected neither to wellbore storage nor skin effect.

Using the reduced variables, listed in Table 4.3.5, the pressure transient response will conform to :

$$p_D = \frac{1}{2} E_i \left( -r_D^2 / 4t_D \right) \quad (4.3.4)$$

The interpretation exercise consists of superposing the pressure vs time log-log plot to type curve  $(-E_i(-u))$  until achieving the best possible fit and deriving reservoir permeability  $k$  (or transmissivity  $kh$ ) and total compressibility  $c_t$  or porosity  $\phi$  from match

point coordinates (in consistent units, Table 4.3.5) :

$$\log \Delta p = \log p_D - \log \frac{2\pi kh}{qB\mu} \quad (4.3.5)$$

$$\log t = \log t_D - \log \frac{kt}{\phi\mu c_t r^2} \quad (4.3.6)$$

The example shown in fig. 4.3.1 addresses a set of type curves including the additional dimensionless wellbore storage coefficient  $C_D$  and skin factor  $S$ , which actually may render the interpretation somewhat ambiguous regarding uniqueness of the solution.

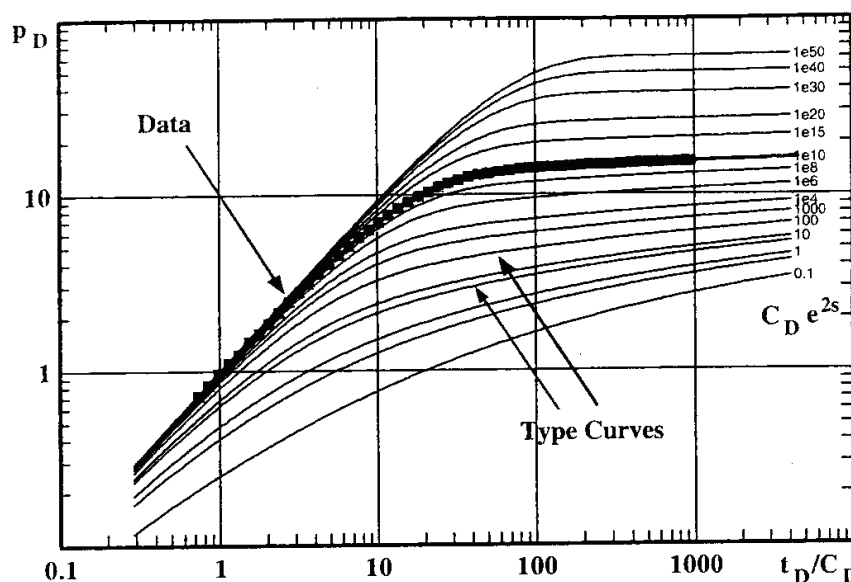


Figure 4.3.1: Log – Log plot – Type curve method (source R.N. Horne, 1995)

- **Semi-log plot straight line analysis**

Regardless of wellbore storage, which can be estimated independently (Horne, 1995) and is elsewhere of moderate interest regarding reservoir analysis, the straight line slope allows to determine both permeability and skin from the following equations.

$$m = 0.183 qB\mu / kh \quad (4.3.7)$$

$$S = 1.151 \left[ \frac{p_i - p_{1hr}}{m} - \log \left( \frac{k}{\phi\mu c_t r_w^2} \right) + 3.23 \right] \quad (4.3.8)$$

- **Pressure buildup**

Previous sections addressed the pressure drawdown stages of well tests.

The superposition principle can be extended to the processing of the pressure recovery stage further to well shut in, leading to :

$$p_i - p_{ws} = \frac{0.183Bqu}{kh} \left[ \log \frac{t_p + \Delta t}{\Delta t} \right] \quad (4.3.9)$$

As a result, the semi-log straight line analysis can be applied to the pressure buildup by plotting pressures  $p_{ws}$  (measured from  $p_{wf}(t_p)$ ) against  $(t_p + \Delta t) / \Delta t$ , known as the Horner plot.

In addition to the  $kh$  product, pressure buildup analysis delivers the skin factor by substitution of the  $\Delta t = 1$  hr pressure :

$$S = 1.151 \left[ \frac{p_{1hr} - p_{wf}}{m} - \log \frac{kt_p}{(1+t_p)\phi\mu c_t r_w^2} + 3.23 \right]$$

The initial reservoir pressure  $p_i$  may also be derived by extrapolating to 1 (infinite  $\Delta t$ ) the straight line fraction of the Horner plot.

• **Well testing summary**

Graphic displays, by means of  $\Delta p$  and  $t_{dp}/dt$  vs time log-log and semi-log plots, form the basis of well test analysis and identification of the reservoir parameters and flow mechanisms involved.

This review is summarised in fig. 4.3.3 semi-log and log-log synthetic representations, which allow to visualise, from early to late elapsed times, wellbore, transient, infinite acting radial flow and boundary effects.

• **Testing chain**

Well tests will usually follow the sequence here after:

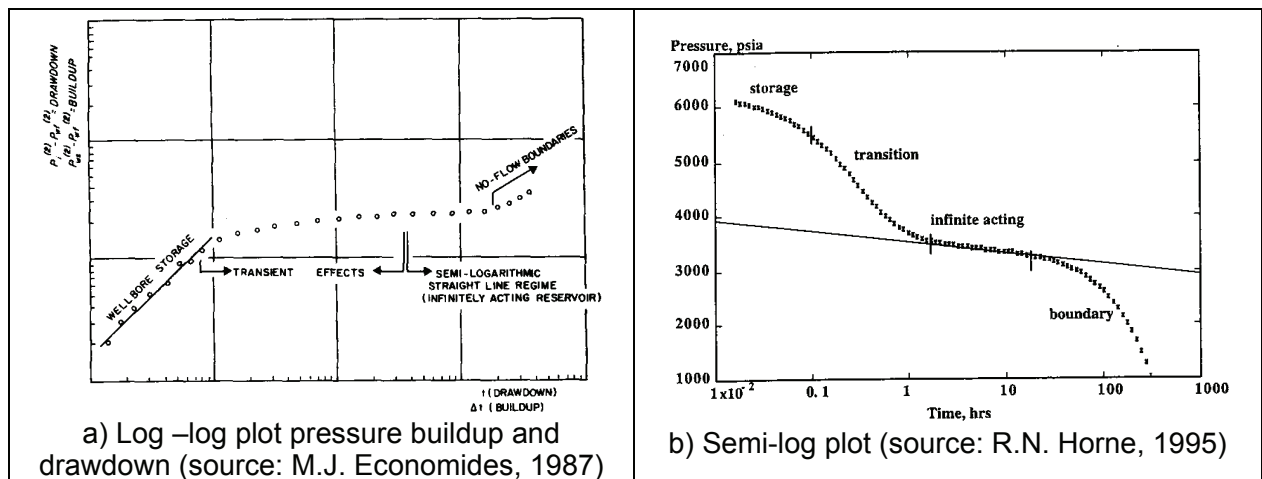
tests while drilling, such as DSTs, aimed at a preliminary assessment of well performance, whenever there is evidence of a reservoir;

short duration tests (24 to 48 hours) following well completion in order to assess well productive (injective) capacity (multirate test) and near wellbore reservoir characteristics (transmissivity and skin);

long duration tests (over a week) to investigate larger reservoir areas and boundary conditions carried out at constant, preferably high, discharge rate;

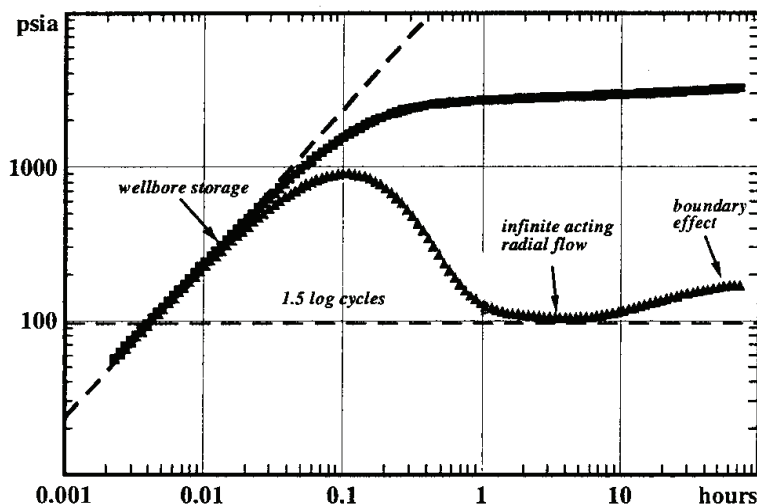
interference tests (several weeks), which will include, in case of geothermal district heating doublet, a production/injection loop circulation test, using surrounding boreholes as observation wells, which, along additional information on reservoir porosity and anisotropy, will provide a database for later reservoir simulation runs.

Tracer testing is frequently associated with multiwell interference testing.



	Early time	Intermediate time	Late time
radial flow	storage	infinite acting radial flow	closed boundary sealing fault constant pressure
fractures	storage bilinear flow	radial flow	closed boundary sealing fault constant pressure
dual porosity	storage	dual porosity behaviour transition radial flow	closed boundary sealing fault constant pressure

c) Time diagnostic of flow behaviour (source: R.N. Horne, 1995)



d) Pressure derivative plot

Fig. 4.3.3: Graphical evaluation of well tests (source: Horne, R.N., 1995)

TABLE 4.3.5 - VARIABLES, EQUATIONS AND UNITS USED IN WELL TESTING

Symbol	Definition	Oilfield units	Metric units
P	Pressure	psi	bar
P <sub>i</sub>	Initial reservoir pressure	psi	bar
P <sub>wf</sub>	Well flowing pressure	psi	bar
ΔP <sub>s</sub>	Skin induced pressure change	psi	bar
q	Production (injection) rate	STB/d	m <sup>3</sup> /hr
r	Radial distance	ft	m
r <sub>w</sub>	Wellbore radius	ft	m
t	Time	hr	hr
B	Formation volume factor	(res vol/std vol)	(res vol/std vol)
C	Wellbore storage coefficient	STB /psi	STm <sup>3</sup> /bar
k	Intrinsic permeability	md	d
h	Reservoir net thickness	ft	m
c <sub>t</sub>	Total compressibility factor	psi <sup>-1</sup>	bar <sup>-1</sup>
φ	Porosity		
μ	Dynamic viscosity	cp	cp
P <sub>d</sub>	Reduced pressure	$\frac{kh (p_i - p_{wf})}{141.2 qB\mu}$	$\frac{2\pi kh (p_i - p_{wf})}{qB\mu}$
t <sub>D</sub>	Reduced time	$\frac{0.000264 kt}{\phi\mu c_t r_w^2}$	$\frac{kt}{\phi\mu c_t r_w^2}$
r <sub>d</sub>	Reduced radius	r/r <sub>w</sub>	r/r <sub>w</sub>
C <sub>d</sub>	Dimensionless wellbore storage	$\frac{5.615 C}{2\pi\phi c_t hr_w^2}$	$\frac{C}{2\pi\phi c_t hr_w^2}$
m	Slope straight line semi-log plot	$\frac{162.6 qB\mu}{kh}$	$\frac{0.183 qB\mu}{kh}$
S	Skin factor	$\frac{kh}{191.2qB\mu} \Delta p_s$	$\frac{2\pi kh}{qB\mu} \Delta p_s$

TABLE 4.3.6 - WELL TESTING GRAPHICAL DISPLAYS (SOURCE R.N. HORNE, 1995)

Flow mechanism	Characteristic	Plot
Infinite-acting radial flow (drawdown)	Semilog straight line	$p$ vs. $\log \Delta t$ , (semilog plot, sometimes called MDH plot)
Infinite-acting radial flow (buildup)	Horner straight line	$p$ vs. $\log \Delta(t_p + \Delta t)/\Delta t$ , (Horner plot)
Wellbore storage	Straight line $p$ vs. $t$ , or Unit slope $\log \Delta p$ vs. $\log \Delta t$	$\log \Delta p$ vs. $\log \Delta t$ , (log-log plot, type curve)
Finite conductivity fracture	Straight line slope $1/4$ , $\log \Delta p$ vs. $\log \Delta t$ plot	$\log \Delta p$ vs. $\log \Delta t$ , or $\Delta p$ vs. $\Delta t^{1/4}$
Infinite conductivity fracture	Straight line slope $1/2$ , $\log \Delta p$ vs. $\log \Delta t$ plot	$\log \Delta p$ vs. $\log \Delta t$ , or $\Delta p$ vs. $\Delta t^{1/2}$
Dual porosity behavior	S-shaped transition between parallel semilog straight lines	$p$ vs. $\log \Delta t$ , (semilog plot)
Closed boundary	Pseudosteady state, pressure linear with time	$p$ vs. $\Delta t$ , (Cartesian plot *)
Impermeable fault	Doubling of slope on semilog straight line	$p$ vs. $\log \Delta t$ , (semilog plot)
Constant pressure boundary	Constant pressure, flat line on all $p, t$ plots	Any

(\*) Not recommended

### 4.3.3 Tracer tests

Tracer testing is a vast domain, whose scope will be restricted here to the main issues relating to geothermal reservoir characterisation, flow mechanisms and water injection.

An early application of tracers was designed by Ramey and Nabor (1954) to estimate the swept reservoir volume between one injection and several producing wells. They derived the following equation, relating tracer detection to swept volumes:

$$c_{\min} = \frac{V_{inj}}{1.076\phi D^2 h}$$

where:

$c_{\min}$  = tracer detection limit ( $t/m^3$ )

$V_{inj}$  = injected tracer mass

$D$  = well spacing (m)

$h$  = net reservoir thickness (m)

$\phi$  = effective porosity

In so doing, the tracer is assumed stable (no decay or long decay period) and non-adsorbed by the swept rock.

Another popular application of tracers aims at tracking the migration of (re)injected reservoir fluids. A series of tests were conducted in the Dixie Valley, Nevada, high

temperature field, as reported by Rose *et al* (1997, 2002). They used fluorescein and naphthalene sulfonate and disulfonate, which proved to be reliable due to their environmentally benign and stable properties at high temperatures and easy detection (fluorescence spectroscopy) at low concentrations (0.1 ppb). In addition, field responses in terms of flow paths, elution curves and breakthrough times were model calibrated via two reservoir simulation codes thus providing the reservoir engineer with optimum design features of future tests.

Similar conclusions were reached on several Philippines and Indonesian fields.

Another attractive application addresses the estimation of the thermal breakthrough time on a geothermal district heating doublet, of the type discussed in a previous section, in order to check whether model predictions match the actual field behaviour. The idea consists of adding a given volume of tracer to the (re)injected water and measure the arrival time of the **hydraulic** front on the production well. This would allow to predict the thermal breakthrough time, bearing in mind that the arrival of the **thermal** front is significantly delayed,

owing to rock/fluid heat transfer, by the following ratio:

$$\frac{\phi \gamma_f}{\phi \gamma_f + (1 - \phi) \gamma_r}$$

In such circumstances, a stable, long period ( $\geq 12$  years), isotope such as Tritium, seems an appropriate candidate. Unfortunately such an experiment could not be carried out on Paris Basin wells.

More sophisticated applications, discussed by Vetter (1981) and Gherghut (2007), use chemically reactive tracers which, absorbed by the rock, might give an estimate of the rock to fluid heat exchange area provided reaction rates do not get affected by pH effects.

There are other, more or less exotic, uses of tracers among which should be mentioned the injection/repumping of either radioactive or chemical tracers in order to detect and localise well casing leaks, discussed by Ungemach *et al.* (2002), a cost effective substitute to conventional packer leak-off tests.

Tracer flow conforms to a solute transport process, mathematically expressed by the following partial differential (dispersion) equation:

$$\left( \overline{D} \nabla^2 c - U c \right) = \phi \frac{\partial c}{\partial t}$$

where  $D$  is the dispersion coefficient (m), which can be added to the heat and mass transfer reservoir simulation codes to appraise solute transport kinetics.

## 4.4 RESERVOIR ENGINEERING

### 4.4.1 Reservoir physics. An Overview

A hydrothermal system meeting the four reservoir prerequisites stated in introduction will host hot fluids, whose physics and chemistry are governed by heat and mass transfer processes and chemical thermodynamics.

Heat flow, the source of geothermal energy, is governed by the Fourier law of heat conduction, which relates heat flow density to the temperature gradient via the heat conduction coefficient of the medium in contact. Similarly, in a porous rock, the soaking fluid(s) will flow at a rate given by the Darcy

law relating the pressure gradient (diminished, in the vertical direction, by gravity) to velocities, via the rock permeability divided by the fluid viscosity. Note here that the Darcy law applies separately to each fluid phase (liquid, vapour) by applying a relative permeability criterion in which phase relative permeability are expressed as a function of liquid saturation.

Note also that capillary effects are usually neglected in practical reservoir simulation studies. Finally, mass flow of the fluid constituents, such as dissolved salts and non condensable gases (principally  $\text{CO}_2$ ) soluble in water, and also in the gaseous phase, will take place, according to the Fick law of molecular diffusion, which relates the mass fraction gradient to mass fluxes, via a combination of a diffusivity factor, porosity, and porous medium tortuosities (Pruess, 2001).

Natural heat convection will occur in the form of convective rolls (Combarnous, 1975) as a result of fluid density changes (buoyancy) at depth and upward heating from bed rocks.

Forced convection will take place, in presence of sources and sinks, and become clearly the driving mass and heat transport mechanism, creating, when amplified by commercial exploitation, an imbalance in the natural field recharge vs well discharge budget, between renewability and exhaustion, a mining issue at the centre of the sustainability debate (Ungemach, 2007; Sanyal, 2005; Rybach, 1999).

Before moving to the derivation of the mass and energy conservation equations, worth mentioning, with respect to the in site fluid states, are the physical properties of the main geothermal fluid, i.e. water under its two, liquid and gaseous, states illustrated in fig. (4.3.1) to (4.4.3).

Figure 4.4.1 evidences in the pressure vs temperature diagramme the phases of pure water and the transition from liquid to vapour across the saturation curve. The latter, also called boiling curve, is displayed in more detail in fig. (4.4.2) for pure water and brines up to 25% (mass) equivalent salinity. Fig. (4.4.3) synthesises in a form more appropriate for thermodynamic calculations, the water phases and transitions.

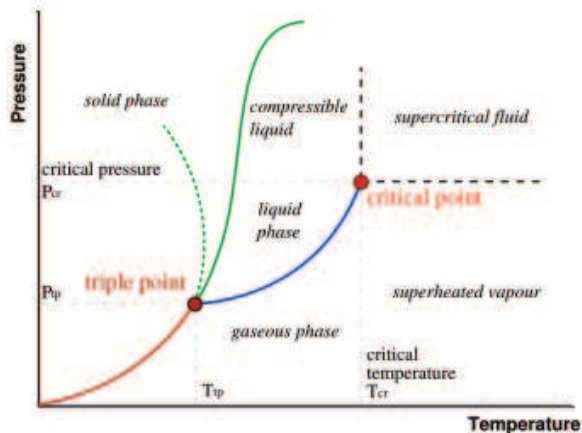


Fig. 4.4.1 – Phase diagramme for pure water.

Figure 4.4.1 evidences in the pressure vs temperature diagramme the phases of pure water and the transition from liquid to vapour across the saturation curve. The latter, also called boiling curve, is displayed in more detail in fig. (4.4.2) for pure water and brines up to 25% (mass) equivalent salinity. Fig. (4.4.3) synthesises in a form more appropriate for thermodynamic calculations, the water phases and transitions (liquid/two-phase/vapour), the pressure, enthalpy relationship (Mollier diagramme) for pure water together with isodensity, temperature and steam quality (mass fraction) contours.

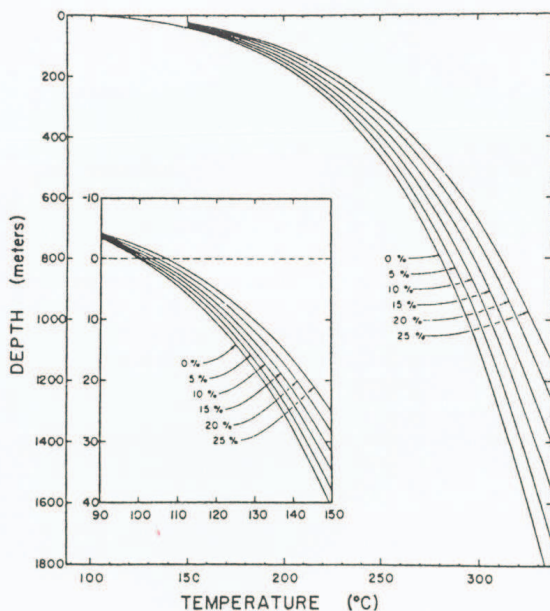


Fig. 4.4.2 – Boiling curves for pure water and brines.

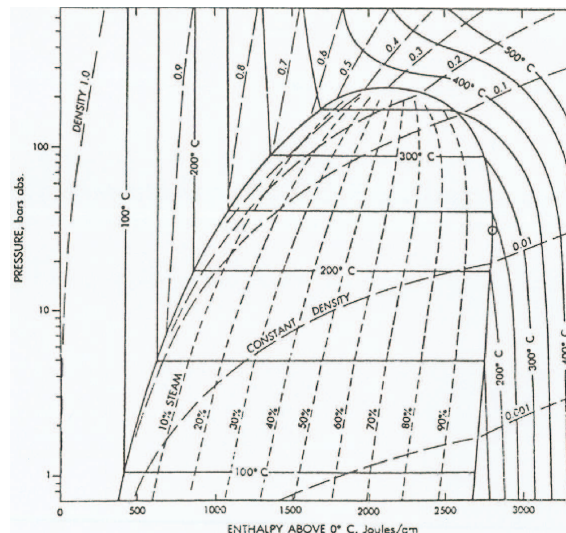


Fig. 4.4.3 – Pressure-enthalpy diagramme for pure water (Mollier).

The quantification of the mass and energy balances leads to a set of partial differential equations (PDE) further illustrated, in discretised forms (finite difference equations, FDE), in section 4.4.3.

#### 4.4.2 Material balance approach

The method, popularised by petroleum reservoir engineers, has been extensively used, in lumped parameter modelling, as a geothermal reservoir evaluation tool.

It assumes that the reservoir behaves as a single, averaging, entity in response to (inner) field production/injection and (outer) peripheral water influx (Gudmundsson, 1988).

Hence, the material balance can be written under a simplified form:

$$W(t) = W_o - W_p + W_i + W_r \quad (4.1)$$

where  $W$  stands for masses and subscripts  $o$ ,  $p$ ,  $i$  and  $r$  for initial in place, production, injection and recharge fluid masses respectively.

Assuming further, that (i) neither water influx nor injection occurs, and (ii) withdrawn fluid mass  $W_p$  can be related to pressure drawdown  $\Delta p$  as:

$$\Delta p = W_p / (\Phi V \rho c_f) \quad (4.2)$$

where  $\Phi$ ,  $V$ ,  $\rho$  and  $c_f$  refer to porosity, reservoir volume, fluid density and compressibility respectively. Note incidentally that heat fluid compressibility may increase by



several orders of magnitude from liquid water, to steam and two phase mixtures.

(4.14) is a straight line,  $Wp$  vs  $\square p$  plot, assuming a constant  $1/\phi V \rho c_f$  slope, an assumption no longer valid for superheated steam reservoirs owing to a strongly pressure dependant compressibility coefficient. The pseudo-reduced natural gas pressure function  $p/z$  ( $z$  = gas deviation factor) is used instead and plotted against the cumulative steam production, an approach pioneered and successfully verified by Whiting and Ramey (1969) and Ramey (1970), the latter on the Geysers field, and illustrated in fig. (4.4.4), which yields, by extrapolating to zero pressure the straight line plot, the initial steam in place mass  $W_0$ .

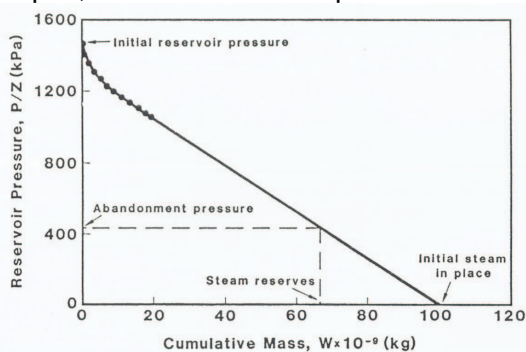


Fig. 4.4.4 – Pressure Mass depletion vs cumulative mass production vapor dominated reservoir (source: Gudmunsson, 1988).

#### 4.4.3 Reservoir simulation

Geothermal reservoir simulation aims basically at solving by numerical techniques the set of simultaneous PDEs and related equations of state and boundary/initial conditions governing the mass and heat transfers in the reservoir in view of (i) checking the consistency of the conceptual model, (ii) assessing reservoir structure, resource status, flow patterns and discharge/recharge mechanisms, and (iii) last but not least, optimising field development in a, preferably, sustainable reservoir management perspective.

Accordingly, it has become, over the past decade, a standard widely used reservoir evaluation tool, whose methodology conforms to the interactive sequence sketched in fig.(4.4.5) flow chart.

It should be readily stressed here that the elaboration of a relevant conceptual mo-

del of the reservoir is, whatever the degree of sophistication of the applied – deterministic vs probabilistic, forward or inversion – modelling techniques, of utmost importance in securing further simulation and assessment stages.

Hence, a reliable interpretation of all field data collected from surface/subsurface geological, hydrogeological, geophysical, geochemical surveys, drilling/logging/testing, tracer tests and their integration into a comprehensive conceptual model, imaging reservoir structure and extent, major flow paths, intake/outflow zones and temperature patterns, is a major consideration for the reservoir engineer.

Natural state modelling and model calibration phases come next. Natural state modelling often requires repeated simulation runs over long periods, several thousands years or more, until the system reaches steady state (see simulation flow chart in fig. 4.4.6). The next step consists of matching model temperature and flow outputs against measured data according to the modelling methodology summarised in fig. 4.4.7.

Interpolation of measured field data (temperature, pressure, enthalpies) and parameters (permeability, porosity,...) is generally performed by means of statistical (Kriging) methods available from routine computer software.

Model calibration is a similar, history matching, trial and error process, carried out under transient conditions provided by well (production, pressure, enthalpy, non condensable gas contents,...) exploitation records. It enables to assess the most consistent field parameter distribution according to a best fit criterion between computed and recorded well data. The latter suggests parameter inversion techniques, widely applied in geophysical data processing, based on minimising of differences between computed vs observed field patterns be implemented instead of the current, somewhat tedious, forward (direct) trial and error parameter adjustment practice. As a matter of fact, most geothermal modellers have resisted so far this appealing trend preferring to rely on physically dependable conceptual and natural state models. They should not be blamed for that.

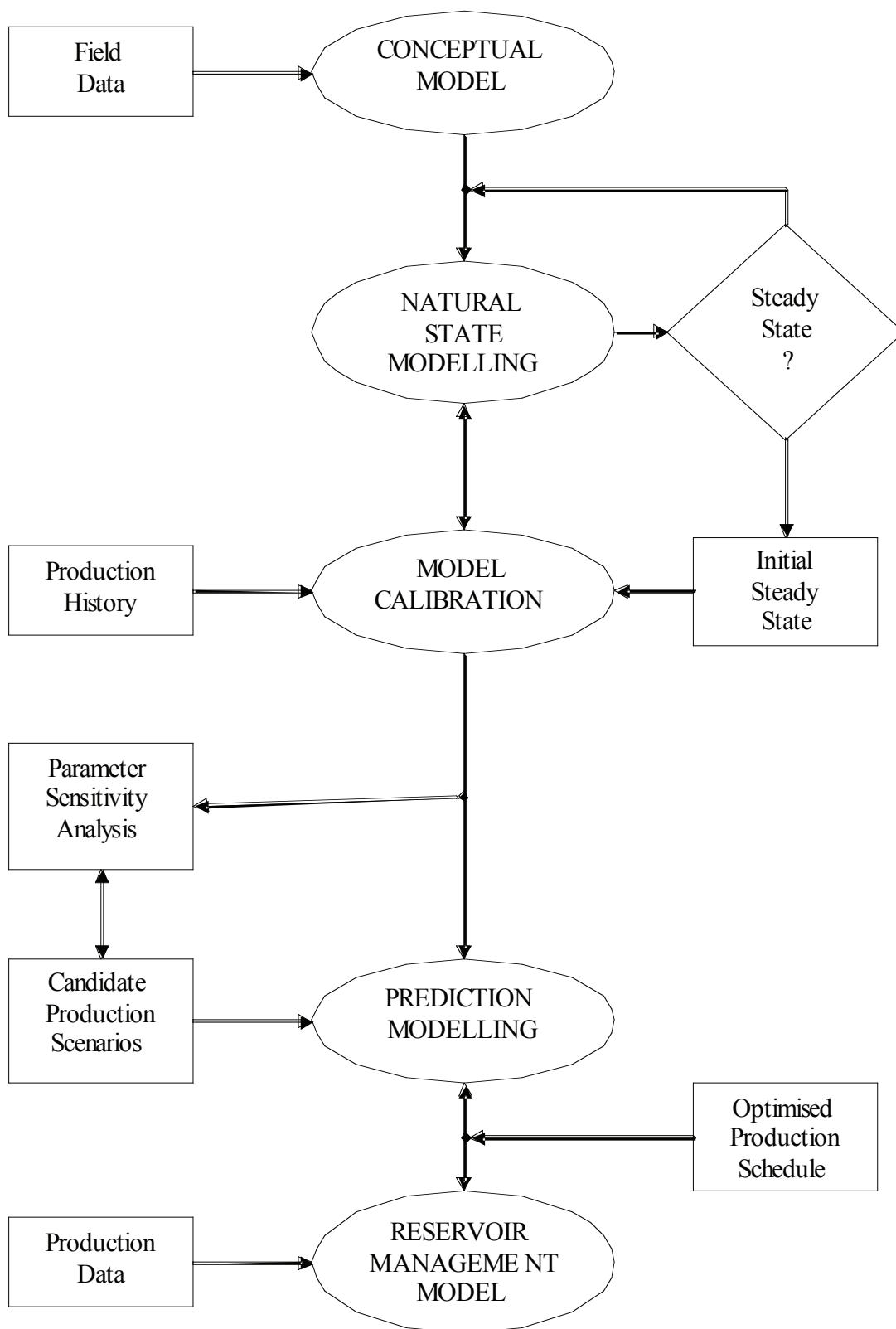


Fig. 4.4.5 – Simulation methodology.

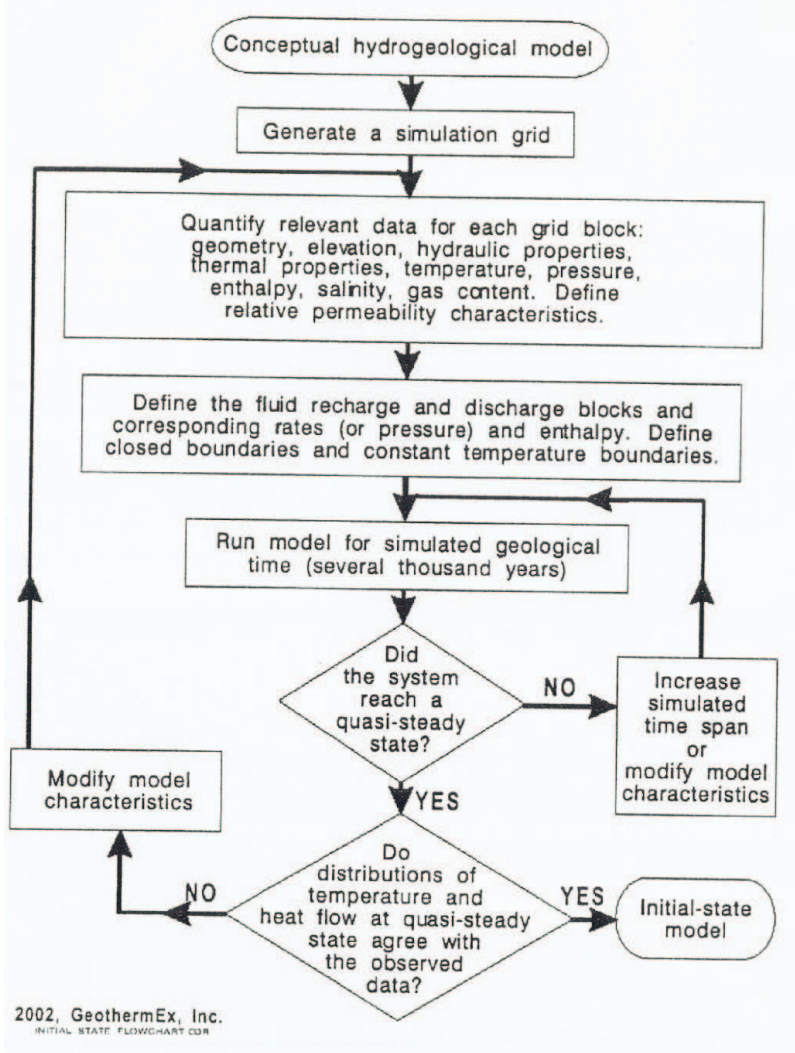


Fig. 4.4.6 – Natural state modelling flowchart (source: Sanyal, 2002).

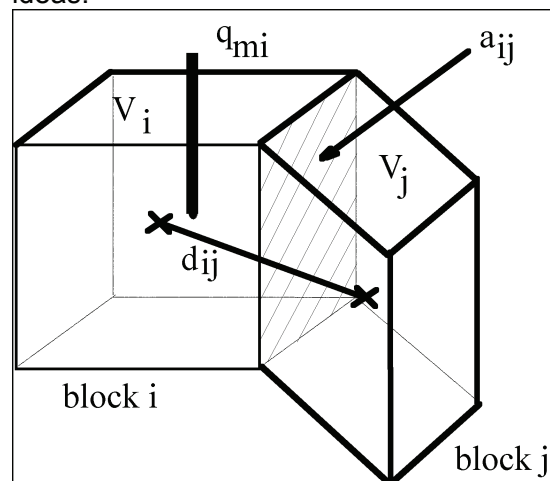
### Numerical modelling

The derivation of the FDEs based on the integrated finite difference approach, is described herein after (Antics, 2005).

It is assumed that the region of interest is divided up into blocks or elements. The  $i$ -th block has a volume  $V_i$  and is connected by an area of  $a_{ij}$  to the  $j$ -th block. This formulation allows for an irregular block structure but includes more regular block structures such as rectangular blocks or polar coordinate systems as special cases.

Here  $p_j^n$  and  $T_i^n$  are used to represent pressures and temperatures in the  $i$ -th block at the end of the  $n$ -th time step. The  $n$ -th time step is of duration  $\Delta t_n$ .

All successful geothermal simulation techniques are based on two common ideas:



1. Difference equations are fully implicit with all mass and energy fluxes evaluated at the new time level.

2. Upstream weighting is used to calculate interface quantities.

The procedure discussed here is block-centered for pressures and temperatures while fluxes are calculated at block boundaries. The discrete mass balance equation can be written:

$$V_i (A_{mi}^{n+1} - A_{mi}^n) = - \sum_j a_{ij} Q_{mij}^{n+1} \Delta t_{n+1} + q_{mi}^{n+1} \Delta t_{n+1} \quad (4.23)$$

Here  $Q_{mij}^{n+1}$  is the mass flux from block  $i$  to block  $j$  evaluated at the end of the  $(n+1)$ th time step. Similarly  $q_{mi}^{n+1}$  is the mass production from block  $i$  evaluated at the end of the  $(n+1)$ th time step (positive for injection).

The production rate  $q_{mi}^{n+1}$  use in equation (1) is a total flow rate (kg/s). Similarly the discrete energy equation is:

$$V_i (A_{ei}^{n+1} - A_{ei}^n) = - \sum_j a_{ij} Q_{eij}^{n+1} \Delta t_{n+1} + q_{ei}^{n+1} \Delta t_{n+1} \quad (4.24)$$

Here  $Q_{eij}^{n+1}$  and  $q_{ei}^{n+1}$  are defined as for the mass equation above.

For discretisation of Darcy's Law the equations below are used:

$$Q_{mlij}^{n+1} = - \left( \frac{kk_{rl}}{v_l} \right)_{ij}^{n+1} \left[ \frac{p_j^{n+1} - p_i^{n+1}}{d_{ij}} - \rho_{lij}^{n+1} g_{ij} \right] \quad (4.25)$$

$$Q_{mvij}^{n+1} = - \left( \frac{kk_{rv}}{v_v} \right)_{ij}^{n+1} \left[ \frac{p_j^{n+1} - p_i^{n+1}}{d_{ij}} - \rho_{vij}^{n+1} g_{ij} \right] \quad (4.26)$$

The total mass flow becomes

$$Q_{mij}^{n+1} = Q_{mlij}^{n+1} + Q_{mvij}^{n+1}$$

$$Q_{eij}^{n+1} = h_{lij}^{n+1} Q_{mij}^{n+1} + h_{vij}^{n+1} Q_{mvij}^{n+1} - K_{ij}^{n+1} \frac{T_j^{n+1} - T_i^{n+1}}{d_{ij}} \quad (4.28)$$

There are several terms in equation (4.25) whose calculation requires further explanation. The gravity term  $g_{ij}$  is the component of gravity acting through the interface. For example,  $g_{ij}=0$  for two blocks

horizontally adjacent, and  $g_{ij}=g$  for two blocks with block  $i$  vertically above block  $j$  the interface densities in the "weight" terms are evaluated using:

$$\rho_{lij}^{n+1} = \frac{1}{2} (\rho_{li}^{n+1} + \rho_{lj}^{n+1})$$

$$\rho_{vij}^{n+1} = \frac{1}{2} (\rho_{vi}^{n+1} + \rho_{vj}^{n+1})$$

The inter-block distance  $d_{ij}$  is the sum of the distances  $d_i$  and  $d_j$  from the centres of the  $i$ th and  $j$ th block to their connecting interface respectively. The interface permeabilities and conductivities are calculated using harmonic weighting and usually they are assumed to be independent of pressure and temperature and therefore need to be evaluated only once at the beginning of the simulation using:

$$\frac{1}{k_{ij}} = \frac{\left( \frac{d_i}{k_i} + \frac{d_j}{k_j} \right)}{d_{ij}}$$

The most important aspect of the interface calculations is the upstream weighting of the mobilities and enthalpies. For example the mobilities are expressed as:

$$\left( \frac{k}{v_l} \right)_{ij}^{n+1} = \begin{cases} \left( \frac{k}{v_l} \right)_i^{n+1}, & \text{for } G_\ell^{n+1} < 0 \\ \left( \frac{k}{v_l} \right)_j^{n+1}, & \text{for } G_\ell^{n+1} > 0 \end{cases}$$

where:

$$G_\ell^{n+1} = \frac{p_j^{n+1} - p_i^{n+1}}{d_{ij}} - \rho_{lij}^{n+1} g_{ij}$$

$$\left( \frac{k_{rv}}{v_v} \right)_{ij}^{n+1} = \begin{cases} \left( \frac{k_{rv}}{v_v} \right)_i^{n+1}, & \text{for } G_v^{n+1} \leq 0 \\ \left( \frac{k_{rv}}{v_v} \right)_j^{n+1}, & \text{for } G_v^{n+1} > 0 \end{cases} \quad (4.27)$$

where:

$$G_v^{n+1} = \frac{p_j^{n+1} - p_i^{n+1}}{d_{ij}} - \rho_{vij}^{n+1} g_{ij}$$

Similarly the enthalpies can be evaluated using the following equations

$$(x_\ell)_{uj}^{n+1} = \begin{cases} (x_\ell)_u^{n+1}, \phi_{op} \Gamma_\ell^{n+1} < 0 \\ (x_\ell)_j^{n+1}, \phi_{op} \Gamma_\ell^{n+1} > 0 \end{cases}$$

$$(x_g)_{uj}^{n+1} = \begin{cases} (x_g)_u^{n+1}, \phi_{op} \Gamma_g^{n+1} < 0 \\ (x_g)_j^{n+1}, \phi_{op} \Gamma_g^{n+1} > 0 \end{cases}$$

The quantities  $A_{mi}^{n+1}$  and  $A_{ei}^{n+1}$  are evaluated as follows:

$$A_{mi}^{n+1} = \phi_i (S_\ell \rho_\ell + S_v \rho_v)_i^{n+1}$$

$$A_{ei}^{n+1} = (1 - \phi_i) \rho_{ii} C_{ii} T_i^{n+1} + \phi_i (\rho_\ell S_\ell u_\ell + \rho_v S_v u_v)_i^{n+1}$$

In these formulae variations of porosity with pressure and temperature could be included by adding the n+1 superscript to  $\phi_i$ . The difference equations (4.23) and (4.24) together with equations (4.25) to (4.39) above are then solved for each time step.

*Input data*

They address the six categories, namely reservoir geometry, formation parameters, boundary/initial conditions, sinks and sources and computational parameters, described in fig. 4.4.9. equations of state

and fluid properties are in general included in the computer programme. It is recommended that a data loading and checking.

*Solving methods*

Clues on numerical analysis of solving linear and non linear systems of FDEs by either direct or iterative techniques may be found in the specialised literature (see for instance Varga, 2000 and Aziz, 1997 the latter more topical with respect to petroleum and geothermal reservoir concerns).

Solutions of non linear systems of the type handled in geothermal numerical modelling applies iterative methods, among which the Newton Raphson technique is the most widely utilised in geothermal reservoir simulation.

**4.5 HEAT EXTRACTION AND PRODUCTION TECHNOLOGY**

**4.5.1 Steam production**

Steam may be produced from either compressed liquid, two phase liquid/vapour or superheated vapour reservoirs. Here, liquid and vapour are referred to water and steam although it should be borne in mind that they often coexist with gases (in particular non condensable) and solids (salts) dissolved in the liquid and vapour phases.

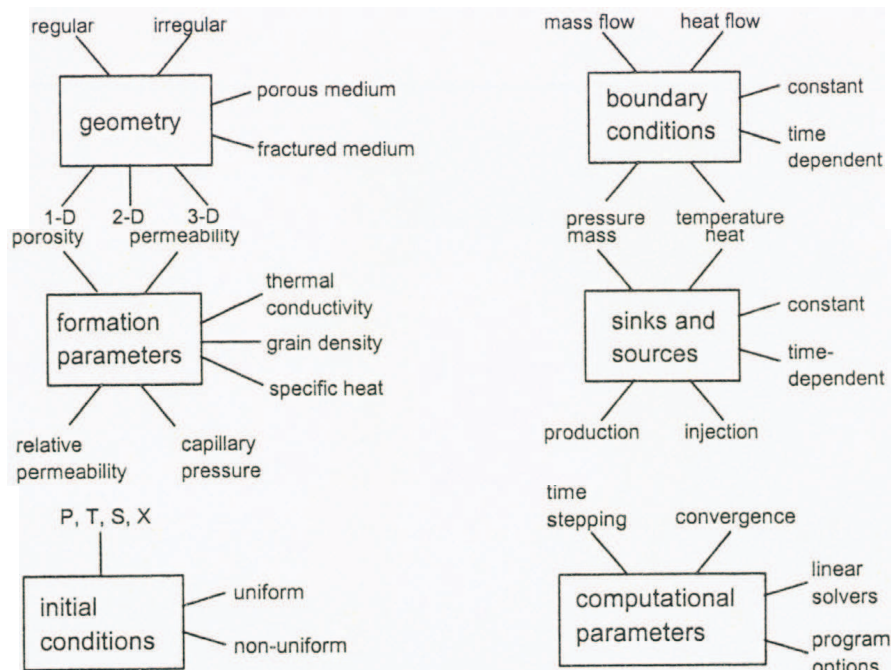


Fig. 4.4.9 – Simulation input data group (source: Pruess, 2002).

Fluid may also change state during production further to pressure depletion. Such is the case of an initially compressed liquid turning two phase as can be noticed from steam tables (Keenan *et al*, 1969).

Energy densities of the rock and soaking fluid states and related volume requirements and energy outputs show the dominant energy contents of the rock and of the fluid respective to the single phase and two phase settings, a situation reflected in table (4.5.1) example which addresses a 250°C reservoir and 40/34 bar initial/final pressures respectively. Here, the advanta-

ges of the two phase reservoir are obvious, from both the energy density and volume requirements stand points. It supplies ca 90% of the total energy content and requires a volume of  $1.5 \cdot 10^9 \text{ m}^3$  to sustain a 30 year life of a 50 MWe rated plant, compared to the  $9 \cdot 10^9 \text{ m}^3$  figure for the single phase (liquid, vapour) cases.

The foregoing have obvious implications on field development of superheated and flashed steam reservoirs when both water injection and make up well issues are implemented to sustain the production objective.

Table 4.5.1 – Energy densities and volume requirements to sustain a 50 MWe rated geoelectric plant over 30 years for various high enthalpy reservoir settings (initial temperature 250 °C; initial/final pressures 40/34 bars; reservoir porosity 15%).

ITEM	Single phase liquid (compressed water)	Two phase liquid/vapor	Single phase vapor (superheated steam)
Total reservoir (rock + density) energy density (kJ/m <sup>3</sup> )	25,170	145,086	23,089
Volume required to sustain a 50 MWe 30 yrs plant life (10 <sup>9</sup> m <sup>3</sup> )	8,844	1,534	9,641

Production of high enthalpy fluids, illustrated in fig. 4.5.1 dual flash condensing cycle schematics, addresses four main issues, in-hole flashing, liquid/vapour separation, non condensable gases handling and waste water disposal.

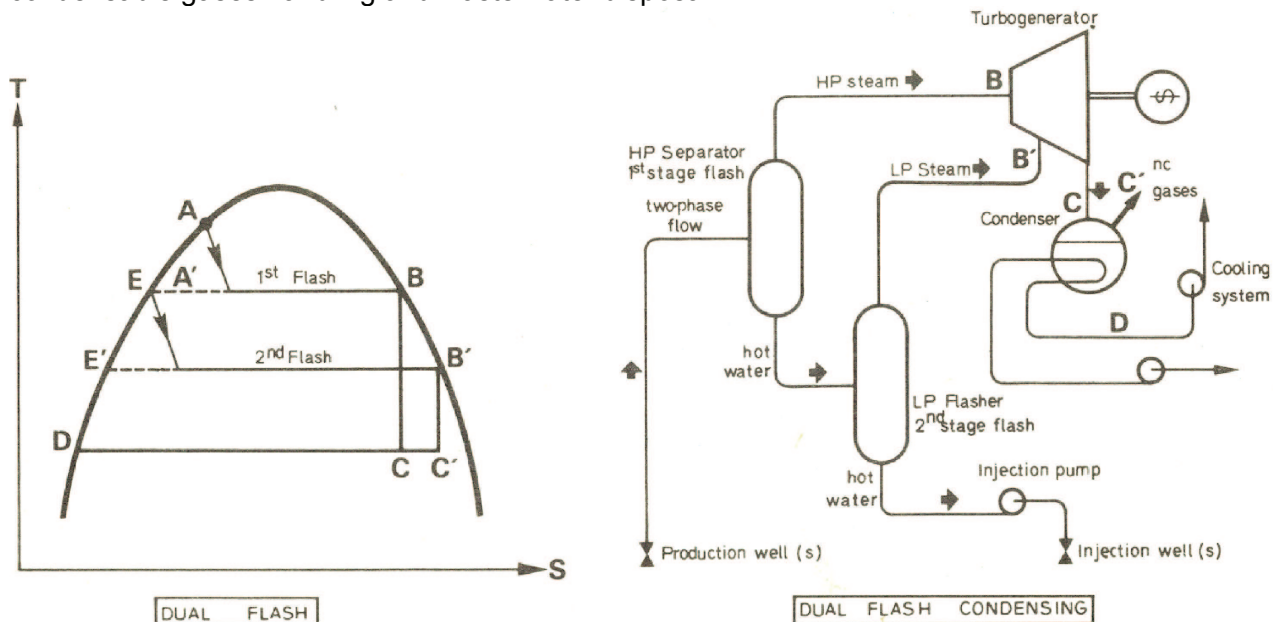


Fig. 4.5.1 – Direct steam expansion and flash cycle. T-S diagrams and schematics (Ungemach, 1987).

*In hole flashing*

Most commercially developed fields are of the liquid dominated type and are likely more to two phase during exploitation above a 230°C temperature cut. Wells are produced in self-flowing mode by vapor lift, as a consequence of in hole flashing, and may achieve productivities in excess of 500 t/h and power capacities nearing 30 MWe (assuming a 40% steam fraction and a dual flash condensing cycle). Note that well bore flashing may cause scaling shortcomings by precipitation, above the flash front, of Calcium carbonates for instance, whenever the well head pressure is depleted below CO<sub>2</sub> partial pressure. In such case the remedial would consist of either increasing well head pressure, at the expense of production losses, or to inject scale inhibitors, preferably stable at high temperatures, below the flash front.

Resources in the 180°C to 230°C range will not exhibit such high well performances due to weaker self flowing/vapor lift capacities and the upper 190°C temperature limit of commercial downhole submersible pumps which readily discards sustained artificial lift production.

Below 180°C, resources, eligible to binary (ORC, Kalina) conversion and combined heat and power uses, are currently produced via downhole lineshaft pumps.

Vapor/liquid separation is completed by cylindrical vessels of either the vertical or horizontal type. Both apply a forced vortex principle. The vertical separator is based on streamlined inlet fluid admission and centrifugal steam separation whereas in the horizontal outfit the fluid enters tangentially and the steam is recovered by gravity. The pros and cons of both separation principles, discussed by Eliasson (2001), tend to favour the vertical separator option which can accommodate a wider pressure range and achieve higher, steam quality and sharper cut off. It further requires limited maintenance commitments. A reasonable compromise would consist of dedicating vertical units to, first stage, high pressure separation and horizontal vessels to, second stage, low pressure separation. The quality of the

steam is controlled by the liquid level in the separator(s). Steam needs to be kept dry, almost 100%, to avoid carry over of water droplets and subsequent mechanical (impact) and chemical (scaling) damage to turbine blades and ancillary equipment.

*Non condensable gases*

Carbon dioxide, a major constituent in geothermal vapor, affects brine thermochemistry turbine efficiency and steam condensing. As a result of fluid flashing, degassing will occur below bubble point pressure, thus decreasing pH, reducing solubilities and generating carbonate scale.

Depending on non condensable gas content two extraction systems may be contemplated, a part from preflashing, ejectors and compressors respectively. Ejectors display poor efficiencies (#15%) and require 12% of the steam mass flow available at well head to extract 1% (vol) of non condensable gases, which clearly restricts their use to low non condensable gas contents.

Higher gas volumes require, because of low inlet pressure, large multistage compressors, with compression rates as high as 8 and high (80%) efficiencies and related costs. Consumption amounts to 3% (mass) of well head vapor flow per 1% (vol) of CO<sub>2</sub> (Ungemach, 1987).

Whenever non condensable gas contents exceed 10% (wt) as recorded in the Monte Amiata field of southern Tuscany (Italy), condensing should be abandoned and back pressure cycles favoured instead.

*Waste water disposal*

Assuming a 250°C, 40 bar fluid pressure, i.e. a single phase compressed liquid state at reservoir conditions, a 7 bar turbine inlet pressure, a 50 MWe rated geoelectric plant with a 20% conversion efficiency, the waste water discharge rate would amount to ca 4200 m<sup>3</sup>/h. Therefore, waste disposal and environmental consequences become a major concern, to which, water injection, seems the most relevant remedial solution.

A superheated steam field would not face such constraints, the sole liquid waste consisting of steam condensates.

Table 4.5.2 – Summary of heat assessments (low enthalpy/direct uses)

<ul style="list-style-type: none"> <li>Heat in place  <math display="block">G(J) = \gamma_t Ah (\gamma_o - \gamma_a) \quad (1)</math>                     where:  <math display="block">\gamma_t (Jm^{-3} k^{-1}) = \phi \gamma_w + (1 - \phi) \gamma_r \quad (2)</math> </li> <li>Recoverable heat  <math display="block">H(J) = \gamma \gamma_t Ah (\gamma_o - \gamma_i) = RG \quad (3)</math>                     where:  <math display="block">R = \gamma (\gamma_o - \gamma_i) / (\gamma_o - \gamma_a) \quad (4)</math> </li> <li>Recovery system efficiency                      since:  <math display="block">H(J) = Q \gamma_w (\gamma_o - \gamma_i)_x t^* \quad (5)</math> <math display="block">\gamma = (Q/Ah) (\gamma_w / \gamma_t) t \quad (6)</math> </li> </ul> <p>Nomenclature :</p> <p>A = reservoir areal extent (m<sup>2</sup>)                      G = heat in place (J)                      H = recoverable heat (J)                      Q = fluid production rate (m<sup>3</sup>/s)                      R = recovery factor                      h = reservoir thickness (m)                      t* = production time (s)  <math>\gamma</math> = volumetric heat (Jm<sup>-3</sup> k<sup>-1</sup>)  <math>\gamma</math> = efficiency of the heat extraction system  <math>\phi</math> = effective reservoir porosity  <math>\gamma</math> = temperature (°C, K)</p>	<p>Subscripts:</p> <p>a = ambient (outdoor)                      i = injection                      t = total (rock + fluid)                      r = rock                      w = fluid (water)                      o = initial reservoir state</p>
---	--

#### 4.5.2 Direct uses

Table 4.5.2 summarises the (in place and recoverable) heat assessments applicable to low enthalpy sources eligible to space and district heating. Equation (6) shows the dependance of heat recovery to the drainage area A; the lower the area the higher the efficiency of the heat extraction system.

##### Numerical application.

$Q = 200 \text{ m}^3/\text{h}$ ,  $t^* = 30 \text{ years}$ ,  $\phi = 0.2$ ,  $\gamma_w = 4.186 \cdot 10^6 \text{ Jm}^{-3}\text{K}^{-1}$ ,  $\gamma_r = 2.143 \cdot 10^6 \text{ Jm}^{-3}\text{K}^{-1}$ ,  
 $h = 20 \text{ m}$   
 $A = 30 \text{ km}^2$ ,  $\eta = 0.15$ ;  $A = 20 \text{ km}^2$ ,  $\gamma = 0.22$ ;  
 $A = 10 \text{ km}^2$ ,  $\eta = 0.33$

Water injection and multi (production/-injection) well arrays represent here the key issue in achieving high heat recovery (Gringarten, 1978, Ungemach, 2007).

The doublet design of low grade heat mining described in fig. (4.5.2), first pioneered in the Paris Basin in 1969 and, since then, extended to the 34 geothermal district

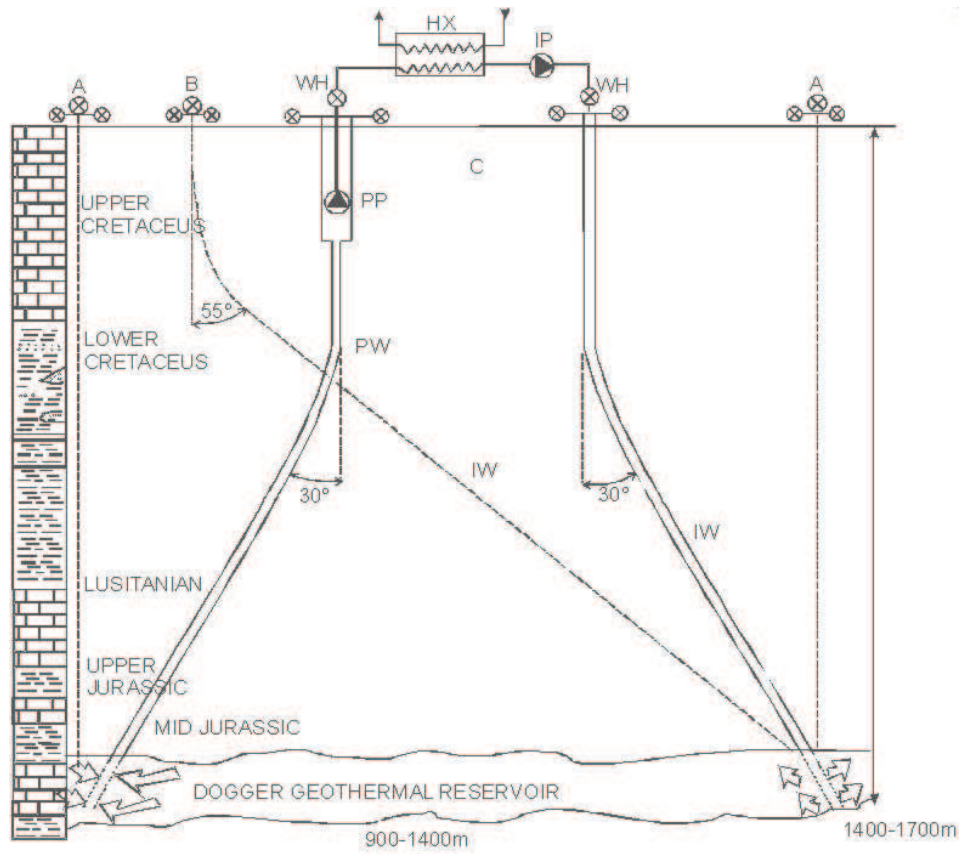
heating (GDH) sites operating to date (fig. 4.5.3) achieves a 25% heat recovery factor against less than 3% for a single well extraction. Five spot arrays of the type practiced in oil secondary recovery water flooding can ambition up to 40% recovery of the heat in place.

Fig. 4.5.4 schematises the design of a GDH system in which the circulation of the geothermal loop may be sustained by either self-flowing or artificial lift.

Self flowing is by far the most attractive production mode provided it can supply target flowrates without excessively depleting well head pressures (i.e. below bubble point), in which case adequate degassing/gas abatement facilities shown in fig. (4.5.5) would be required.

Therefore artificial lift is most often the rule in geothermal, low grade heat, direct uses. It is best achieved thanks to the three submersible pumping alternatives, lineshaft, electrosubmersible, turbine respectively, whose principles are illustrated in figure 4.5.6.





- A - two vertical wells
- B - 1 vertical, 1 deviated
- C - two deviated wells

- PP production pump
- IP injection pump
- HX heat exchanger
- PW production well
- IW injection well
- WH wellhead

Fig. 4.5.2 – Geothermal district heating doublet configurations.

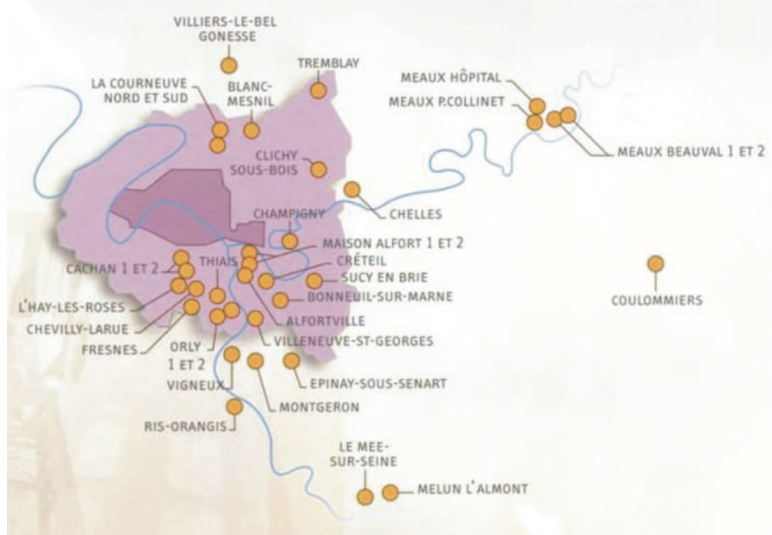


Fig. 4.5.3 Paris Basin operating geothermal district heating doublets (source: ADEME, BRGM, 2007).

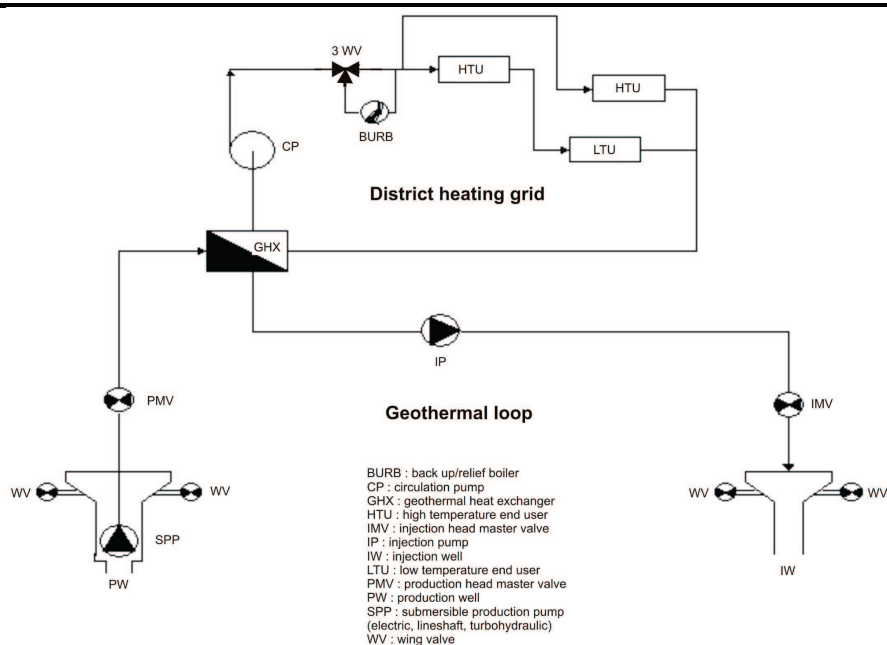


Fig. 4.5.4 Schematic of a submersible pump sustained geothermal district heating doublet (source: GPC IP, 2006).



Fig. 4.5.5 Solution gas degassing/abatement facility (source: GPC IP, 2002).

Doublet bottom hole spacing  $d$  is designed to avoid premature cooling of the production well by assigning a 20 to 25 year temperature breakthrough time  $t_b$  (assuming convective flow alone) from the following

$$\text{formula: } t_b = \frac{\Pi \gamma_t d^2 e}{3 \gamma_f q}$$

Where:

$e$  = reservoir thickness

$q$  = flowrate

$\gamma_t, \gamma_f$  = reservoir and fluid heat capacities

Lineshaft pumps (a), widely used in

ground water production, are quite popular in Iceland and in the Western United States. The well head installed, motor drives an in hole multistage centrifugal pump via a shaft/bearing assembly enclosed in a slim diameter tubing housing in which a make up lubricating fluid is circulated. Icelanders have solved the severe material abrasion problem, caused by silica originated waters, by substituting teflon to metal alloyed bearings. The nature of the lubricating fluid (either mineral oil or make up water), which is, unless recycled, lost in the formation, may be a problem in sensitive environments (mineral waters, thermal baths, medicinal uses).

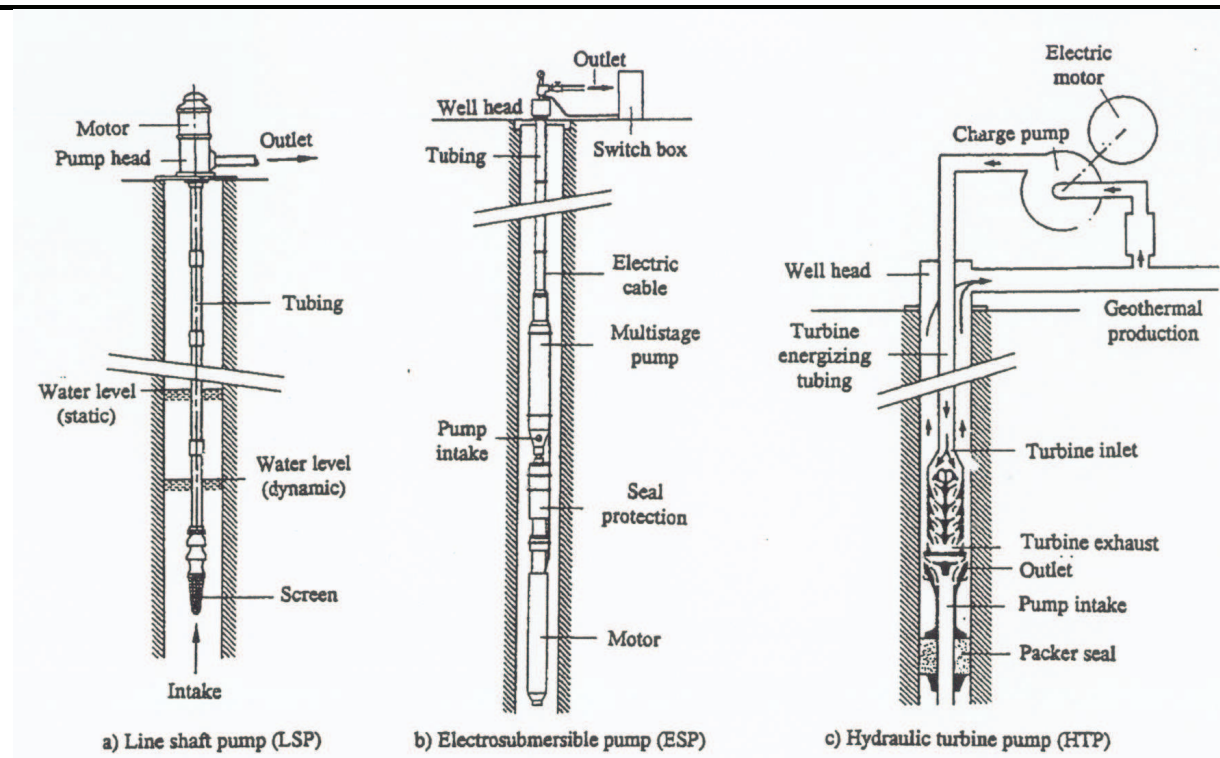


Fig. 4.5.6 - Downhole production pump types.

Many operators rely on electrosubmersible pump sets (b). The technology, derived from the oil industry whenever formation temperatures are in excess of 50°C, consists of submersing in hole the complete multistage centrifugal pump, protector seal and motor (induction squirrel cage type), electric cable string. A degassing outfit may be added in case of high solution gas (GWR) contents. Material definition, seal protector efficiency and motor/cable insulation are the critical problem areas faced by this technology.

Turbine pumps apply a hydraulic motor concept (c). A surface, high pressure, charge pump actuates, via an injection tubing, a down hole turbine driving a single stage centrifugal pump whose intake and outlet are isolated by a packer seal. According to this design, both turbine exhaust and pump outlet fluids are mixed/produced through the energizing tubing/pumping chamber casing annulus and part of the geothermal fluid recycled through the charge pump. Only three district heating wells (two in the Paris basin, one in the Hampshire basin), apply this technology which could be regarded as a, fairly exotic, curiosity.

All three sustained production concepts

exhibit reliable operation records with life-times close to if not higher than five years in hole continuous service. Pros and cons may be summarized as follows.

#### 4.5.3 Heat pumps and borehole heat exchangers

Exploration of low to very low shallow heat resources is exemplified in fig 4.5.7 with two candidate designs ground source heat pump (GSHP)/borehole heat exchangers (BHG) and groundwater well doublets respectively.

GSHPs have a limited capacity of ca 50 W/m which means that a 200 m deep BHE will supply no more than 10 kWt which is sufficient for heating and cooling a large individual home. For larger heat demands a balance should be made between GSHP and ground water well completion costs bearing in mind that GSHP unit cost stand at ca 60 €/m (@ 2007) which, for a 150 kWe capacity would render the concept merely uncompetitive vis-à-vis a ground water doublet completed at 100 m depth. The layout of such a ground water heat pump system, designed for the dual aquifer completion mentioned in section 4.2 is described in fig. 4.5.8.

Pump type	Pros	Cons
LSP	No electric parts in hole. Higher efficiency (surface motor). Long lifetime. Withstands high temperatures. Attractive costs.	Depths limited to 200 m. Delicate handling (installation/removal). Definition of enclosing tubing coating and bearing materials.
ESP	High submersion depths. Long lifetime. High flowrates in limited casing TD's (250 m <sup>3</sup> /hr in 9"5/8). Withstands high temperatures. Solution gas handling (in hole separator). Worldwide service facilities.	Lower efficiency. Electric insulation shortcomings. Higher costs.
HTP	Very long lifetime. No electric parts in hole. Withstands very high temperatures.	Low efficiency (additional energy conversion item). Large diameters (OD's) required. Packer anchoring problems. High costs. Limited manufacturing/service facilities.

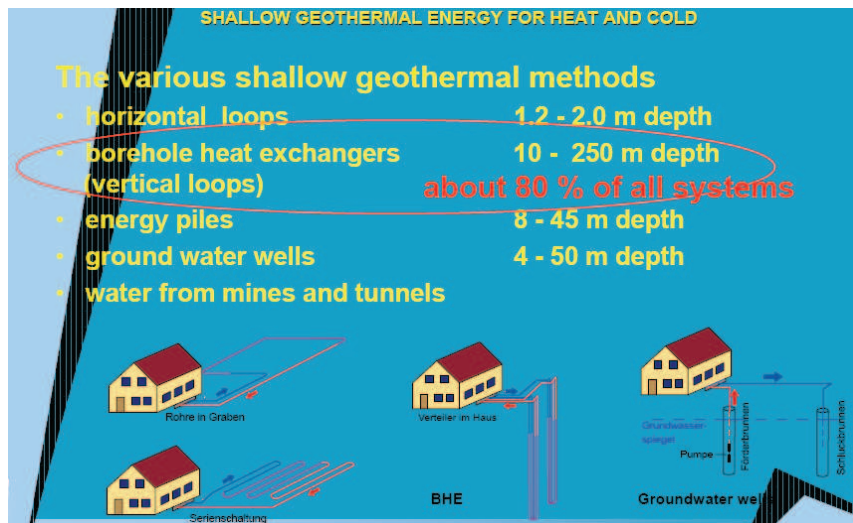


Fig. 4.5.7 – Geothermal heat pump designs (source : Sanner, 2006).

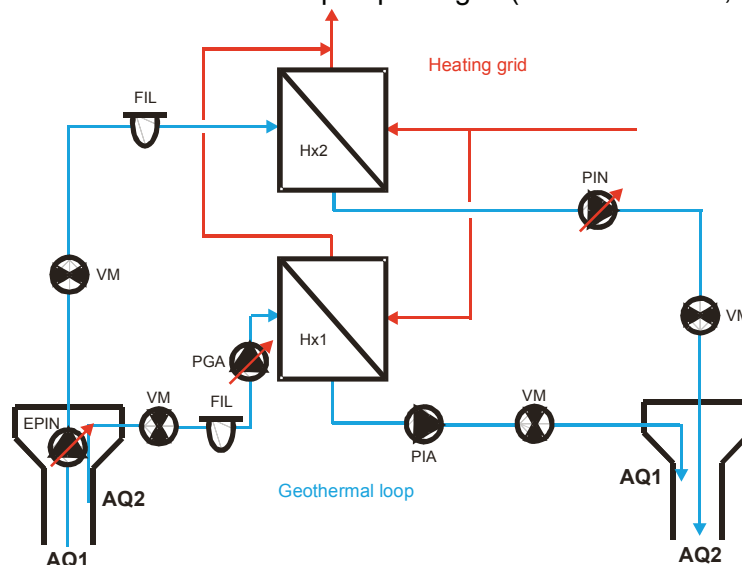


Fig. 4.5.8 – Ground water heat pumps. Pumping/heat exchange layout. Dual aquifer completion (GPC IP, 2007).

However, GSHPs may accommodate large demands whenever they address heating/cooling systems of the type summarised in fig. 4.5.9 schematics and AC options would then be combined with shallow depth building piles, leading to the

Pier concept described in fig. 4.5.10, which may include as many as 350, shallow depth (35 m), large diameter (>1000 mm), BHEs, in which case mining cost can be kept low and the system competitive likewise.

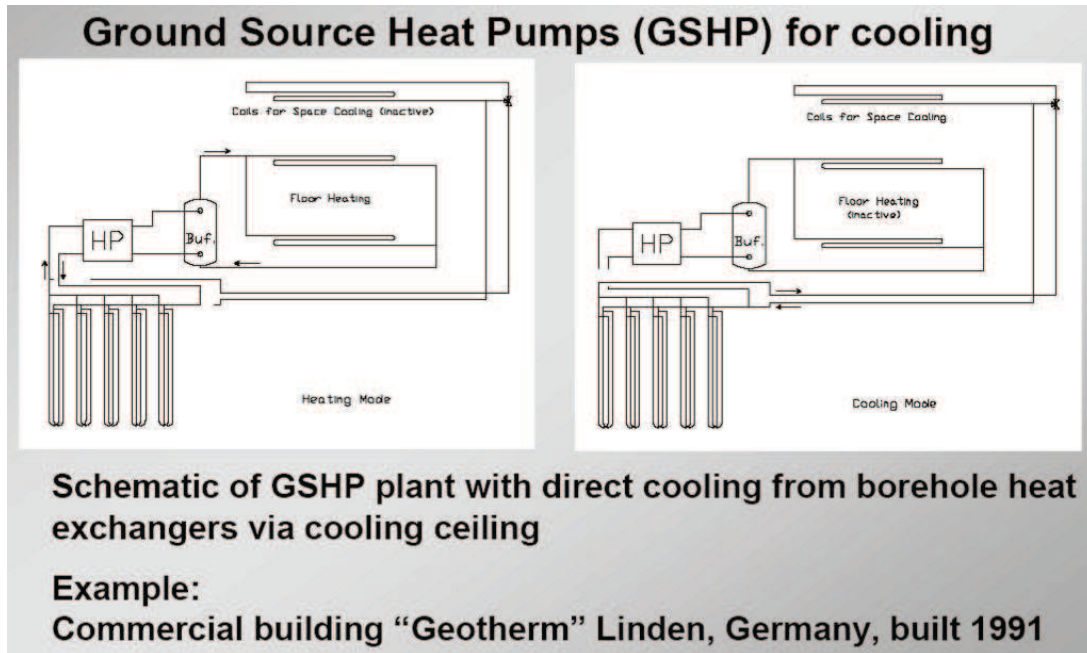


Fig. 4.5.9 – GHSP design for heating/cooling (source: Sanner, 2006).

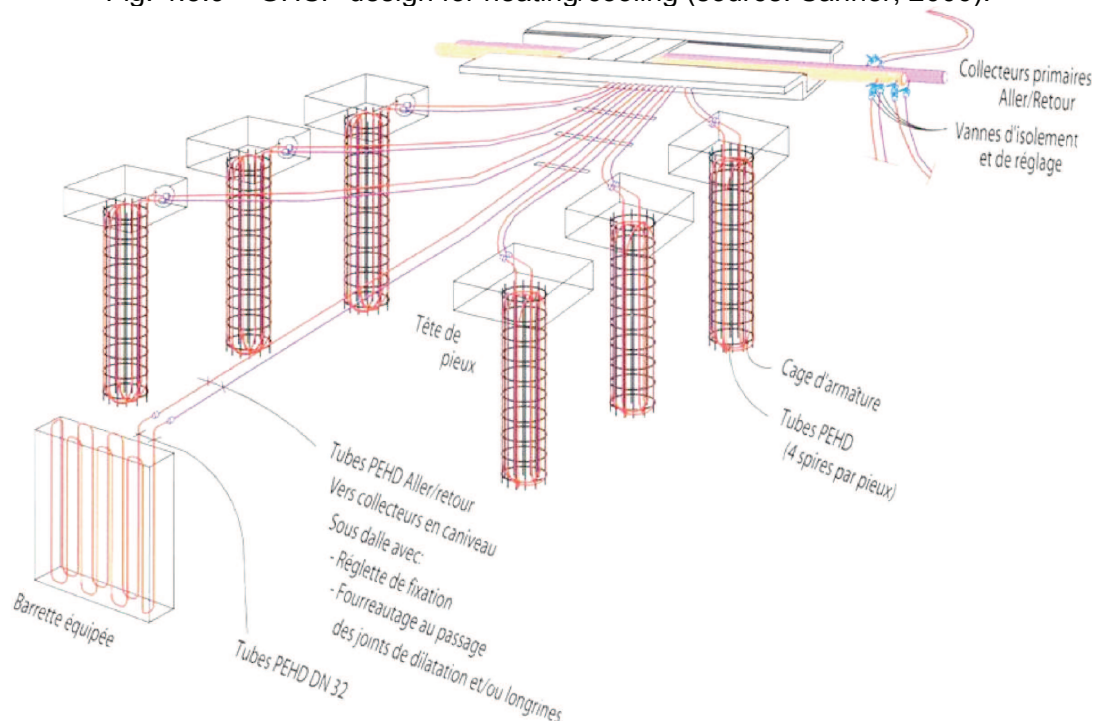


Fig. 4.5.10 – Pier type concept (source: ADEME, BRGM 2005).

#### 4.6 WATER INJECTION

It has been shown, in the previous section, that injection of the heat depleted brine in a compressed liquid, low enthalpy, reservoir could increase by one order of magnitude the heat recovery factor. This could be achieved by sweeping the heat stored in the rock which, in that peculiar setting, was three times higher than that stored in the soaking fluid. For a vapour dominated field this ratio, even when considering absorbed water, stands an order of magnitude higher.

Water injection exhibits, in addition, several other advantages:

- disposal of the waste, cooled, brine, a major concern owing to, increasingly stringent, environmental regulations;
- pressure maintenance as exemplified by the, mass conservative, doublet concept of heat extraction;
- permeability enhancements of high enthalpy reservoirs further to cold water

injection and thermally induced stresses (thermal stress cracking);

- land subsidence control.

These advantages are counterbalanced by:

- fast thermal breakthrough and premature cooling of production wells, a critical issue particularly acute in fractured rock environments;
- triggering of microearthquakes, known as induced seismicity, long noticed in high enthalpy fields and thoroughly analysed by Mossop & Segall (2005), which could actually be turned into an asset by releasing stresses accumulated in seismically active areas thus preventing the advent of presumably devastating earthquakes (Van Poolen and Hoover, 1970).

Waste water disposal has obviously been, and still remains, the primary objective of geothermal operators.

The fast pressure depletion noticed in the Geysers and Larderello vapour dominated fields portrayed water injection as an attractive means for sustaining steam production.

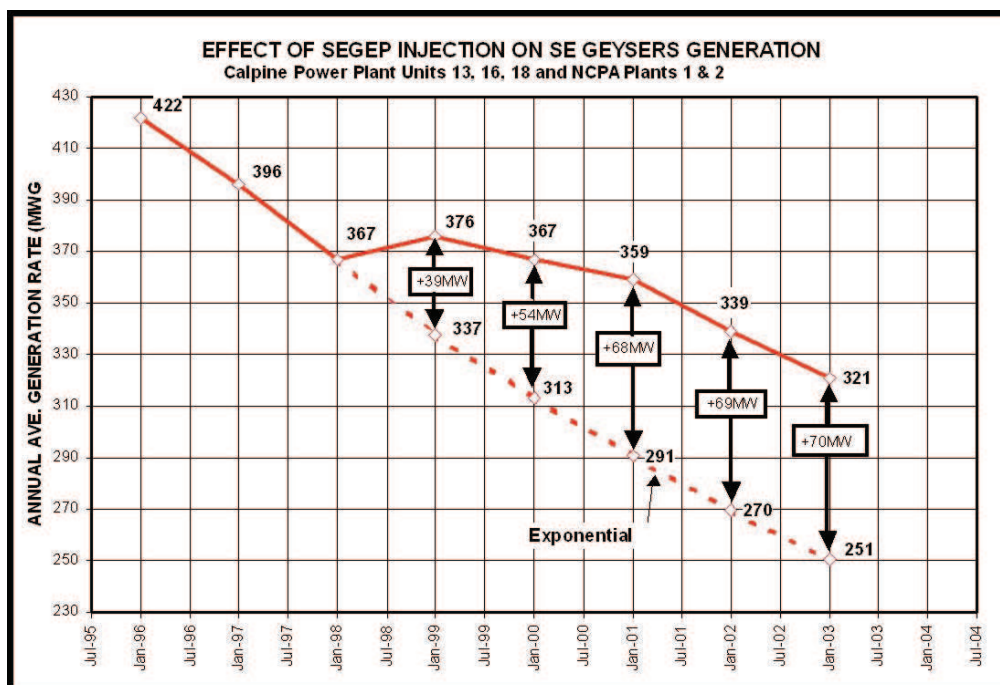


Fig. 4.6.1 – Impact of water injection on SE Geysers power plant (source: Calpine, NCPA).

The Geysers dry steam field had long undergone anarchic over-production, resulting in sharp pressure decline and generated

power losses alike, a trend illustrated in fig. 4.6.1, until water injection came into play. In a dry, superheated, steam field, injection of

the steam condensate, recovered downstream from the turbine outlet, is of limited interest. Therefore an exogenous water source is required which, in the case of the Geysers field, is supplied by a distant (Lakeside) city processed waste water, piped to selected peripheral wells. The impact of water injection can be visualised in fig. 4.6.1. The fast depleting pressure trend has been countered and significant power gains achieved, restoring up to 88 % of the electricity generation level recorded prior to water injection. Identical trends have been noticed in the Larderello field since similar practices were implemented (Capetti, G., 2004).

As far as flashed steam, liquid dominated, fields are concerned, water injection, although raising wider interest from operators, still remains a largely unexplored route. This attitude is likely due to well short-circuiting/premature cooling, injection well plugging, and, last but not least, to induced seismicity fears among others. It somewhat persists in spite of the positive impacts reported in the Imperial Valley of Southern California, despite a locally hostile thermochemical environment, to defeat subsidence of an extensively irrigated farmland, and in the Kizildere and Balçova fields of Western Anatolia (Serpen and Aksoy 2005).

Liquid dominated, high enthalpy, reservoirs are often limited in size and fluid circulation is governed by prevailing fractured porosity/permeability patterns. Therefore, water injection is subject to channelling along preferential flow paths and subsequent short circuiting of production wells.

These distinctive features of fractured geothermal reservoirs led Bodvarsson (1969) to recommend that injection wells be drilled at least one kilometre apart and the water injected several hundred meters below the exploited reservoir. This obviously poses the problem of the injectivity of this deeper horizon which is not known beforehand.

The large majority of low enthalpy reservoirs, eligible to direct uses, belong to sedimentary environments as opposed to high enthalpy, liquid dominated, volcanotectonic settings.

The critical problem area deals with the

injection of cooled brines into fine grained clastic sedimentary reservoirs alternating sand, sandstone and clay sequences. If not carefully designed, injection practice may turn into a disaster caused by non-compatible, formation vs. injected, waters, external/internal particle entrainment, capture and release leading ultimately to well and formation, often irreparable, damage.

As stressed by Ungemach (2003), suspended particles of either (or both) external (carrier fluid) or (and) internal (matrix) origins represent the main permeability impairment risk to well and formation integrities (fig. 4.6.2). As a result, in designing water injection systems in such environments, emphasis is to be placed on low velocities, particle characterisation, filtering criteria and facilities, fluid processing and, last but not least, sound well completion (screen and gravel pack) achieving slow flow injection of, particle free, waters thus securing long well life.

### Examples

#### (i) Particle induced damage

- Modelling strategy

A sound appraisal of, particle induced, formation damage and plugging kinetics implies that transport processes be modelled from microscopic (pore) to macroscopic (near and distant well bore) scales (European Commission, 2001).

- Field test

Two vertical wells, 1200 m apart, were drilled west of Paris in the early 1980s, intersecting a roughly 50 m thick interbedded sand, clay and gravel sequence of Lower Triassic age, displaying net pays of 23 and 32 m, respectively; the wells were completed by wire wrapped screen and gravel pack assemblies. Only part of the annular space was gravel packed in well 1. Production and injection tests were carried out in both wells at constant flow rates of 130 and 120 m<sup>3</sup>/h. The injectivity testing sequences plotted in fig. 4.6.5 demonstrate two constrained pressure transients.

An abrupt pressure drop was noted in well 1, fast stabilising to a steady state injection regime and an injectivity index twice as high as the (temperature corrected) productivity index monitored previously. This

behaviour suggested the build-up, during injection, of a mechanical damage caused by the upward motion of clay particles in the partly gravel packed annulus, resulting in the formation of an external filter cake bridging the pore entries at the sandface.

This diagnosis could be validated by the highly positive skin factor that was obtained from fall off test data, which was restored to its initial negative value after removal of the cake by backwashing.

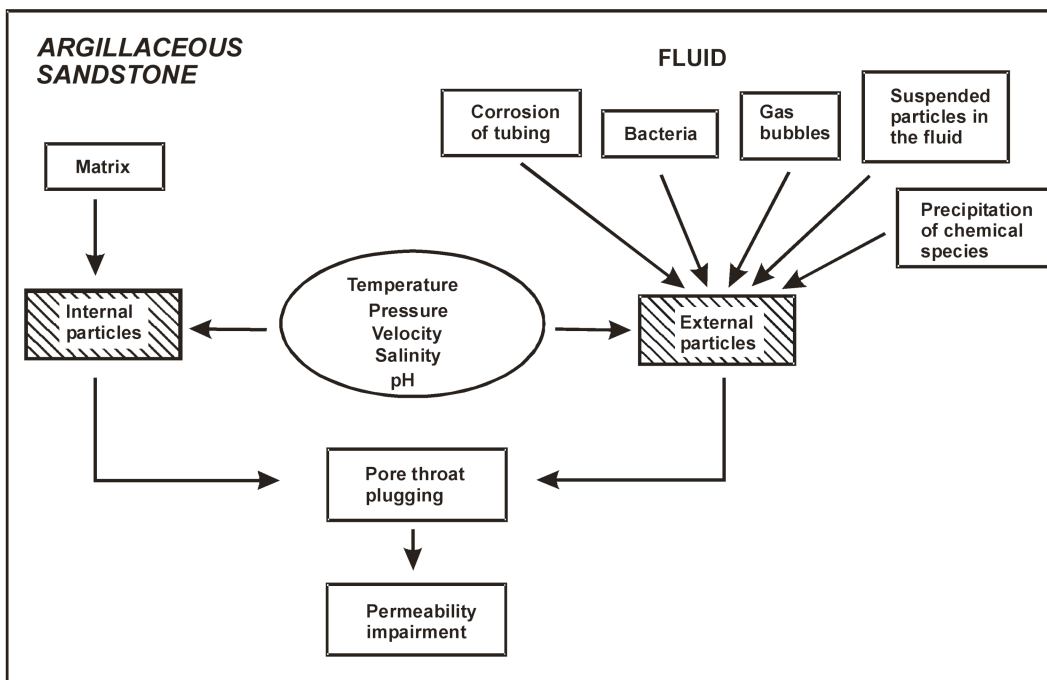


Fig. 4.6.2 – Permeability impairment induced by particles (source: European Commission, 1997).

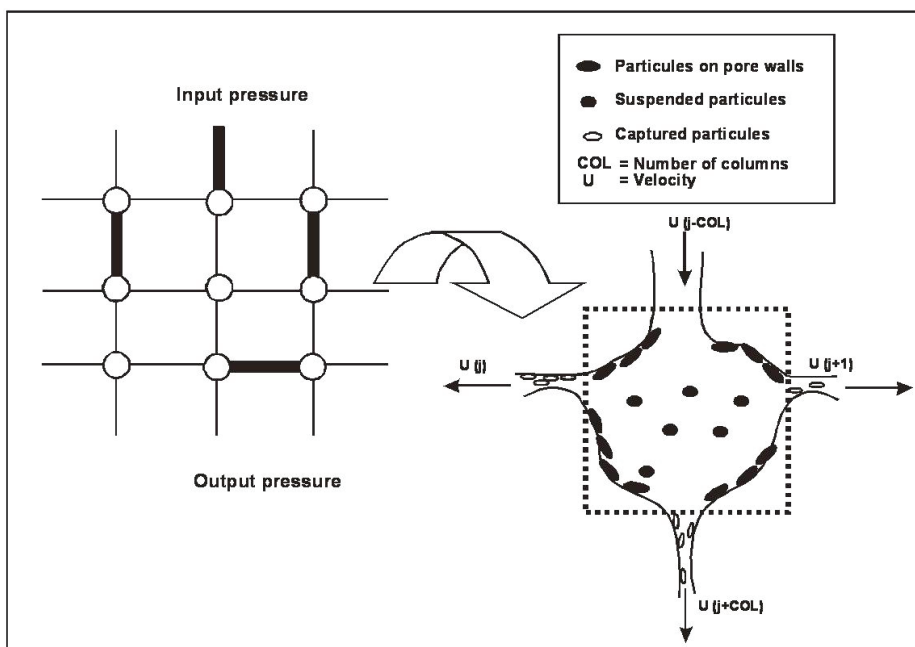


Fig. 4.6.3 – Particle induced damage. Field test. Paris basin Traissic sandstone (source: Ungemach, 2003).



Bottomhole pressures in well 2 did not stabilise at all after 21 h pumping and a dramatically decreasing injectivity trend.

High injection pressures (in excess of 100 bars at well head) and invasion by micrometric size particles were identified as the major damaging factors. Indeed, particle monitoring via millipore filters showed that the concentrations in solids, in the 3 to 5  $\mu\text{m}$  range, decreased by one half whereas in the 0.2 to 1  $\mu\text{m}$  (colloidal) domain they had undergone a two fold increase. Moreover, the sandface inflow velocities, close to 10 cm/s, widely exceeded the 1 cm/s empirical threshold set by the industry.

The foregoing highlight the importance of particle filtering and well completion in the design of water injection undertakings.

#### 4.7 ENHANCED GEOTHERMAL SYSTEMS (EGS)

The EGS route is a continuation of the former hot dry rock (HDR) concept of heat mining initiated in the 1970s. HDR raised considerable interest, at the time, since it suggested that man made geothermal systems could ultimately allow to extract terrestrial heat irrespective of the site specific limitations inherent to natural sources, that is, almost anywhere by-passing thus far the resource mining rationale. The idea got supported by early designs, which assumed deep seated rocks to conform to somewhat ideal elastic bodies, in which two wells, drilled sufficiently deep, would be connected via a large single penny shaped crack by hydraulic fracturing. This doublet system, in which injected cold water, once heated up, would be produced by thermosiphon (buoyant flow) could sustain a 50 MWt capacity over twenty years, provided the fractured heat exchange area be as large as 1 km<sup>2</sup>.

Pilot field experiments, pioneered at Fenton Hill, USA (Los Alamos Labs) and Cornwall UK (Camborne School of Mines) led to more realistic views and designs. Both experienced the difficulty of achieving a multiple well to well connection by volumetric fracturing of a rock mass exhibiting two distinctive fractures (i) natural, pre-existing, fractures/joints, generally misaligned respective to the maximum horizontal *in situ* stress, and (ii) an isotropic *in situ* stress

field and rock strengths. Actually, fracture propagation is governed by shearing and self contained by in situ stresses.

Summing up, these field tests showed the difficulties of reconciling shear propagation of fractures with limited fluid losses and low resistance (hydraulic impedance) to flow of the connecting fracture network, highlighting the so-called HDR paradox.

Anyway, these projects ought to be regarded as large scale rock mechanics experiments providing unvaluable scientific and engineering information with respect to basement rock mechanics, stimulation procedures and fracture mapping techniques.

They favoured the launching of several EGS projects ongoing in France, Germany, Switzerland, USA, Japan, Australia, of which the Soultz one, in Northern Alsace (Rhine Graben), has reached the more mature stage.

According to Garnish (2002), who elsewhere gave a comprehensive review of the EU HDR/EGS R&D status, the critical parameters for success of any EGS venture stand as:

- Hydraulic impedance  $\leq 0.1 \text{ Mpa}/(\text{kg}/\text{s})$
- Water losses  $\leq 10\%$
- Stimulated volume  $> 200 \cdot 10^6 \text{ m}^3$
- Heat exchange area  $> 2 \cdot 10^6 \text{ m}^2$
- Flow rate = 50-100 kg/s

The Soultz EGS project is portrayed in fig. 4.7.1 artist view. It involves three wells, GPK1, GPK2 and GPK3, drilled at 5000 m depths and 200 °C bottomhole temperatures, in crystalline basement rocks underlying a, 1500 m thick, sedimentary cover (fig. 4.7.2). It is targeted at circulating, after due hydraulic stimulations, 100 kg/s of make up water via a single injector (GPK3) and dual producer (GPK1, GPK2) triplet well array, to drive a 6 MWe rated ORC turbine. A view of the circulation test facility is shown in fig. 4.7.3. Well tests demonstrated productivities below expectations, but encouraging in the sense further hydrofrac and mild acid treatments increased well performance which persisted long after, which was perceived as an evidence of self propping of active fractures. An intermediate, medium term, circulation test at ca 100 l/s is foreseen together with the installation of a prototype 1.5 MWe rated ORC plant.

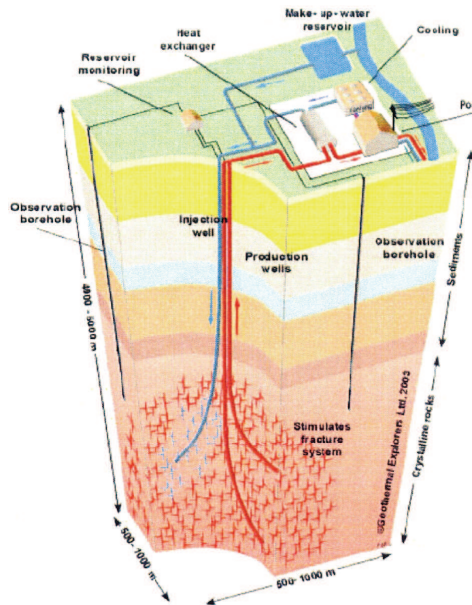


Fig. 4.7.1 - The Soutz EGS project. Artist view (source: ENGINE, 2006).

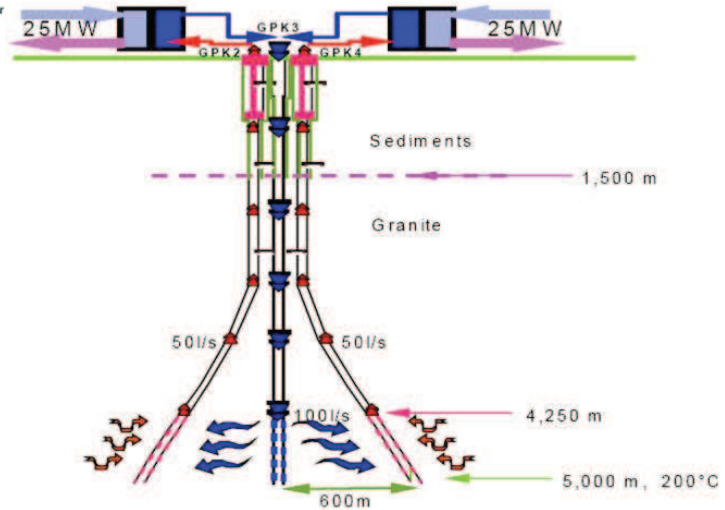


Fig. 4.7.2 – Soutz EGS project schematics (source: BRGM/ADEME 2004).



Fig. 4.7.3 – Soutz EGS project. Circulation test facility (source: ENGINE, 2006).

The project acted as a stimulus for advanced research in the fields of microseismic monitoring/prediction and interactive hydromechanical modelling of fracture propagation and associated, shear triggered, microseismic events (Kohl and Mégel, 2004, Bruel, 2004).

Future development of EGS prospects can be envisaged in selected areas exhibiting eligible tectonic and thermal attributes (see European EGS resources mapped in fig. 4.7.4), provided the seismic risk be overcome.

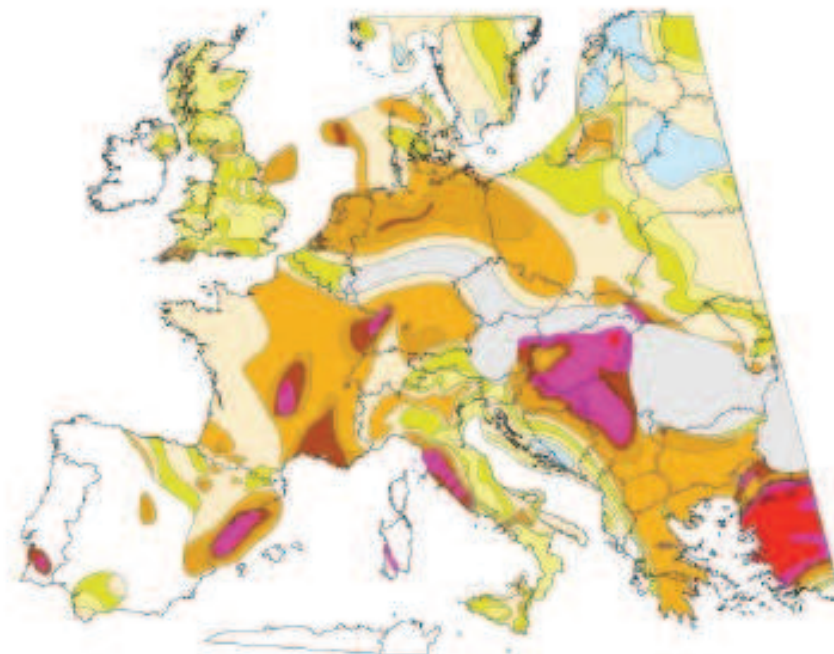


Fig. 4.7.4 – Eligible European EGS potential (source: Genter, BRGM, 2006).

Induced seismicity, a major contributor to fracture mapping and stimulated bulk volume estimates, may also prove a sensitive issue regarding social acceptance whenever the magnitude of induced events passes the human detection thresholds. As a matter of fact, magnitudes above  $M=3$  have been recorded in several instances at Soultz and Basel. Although the physical damages were minimum, if not insignificant, they provoked public reactions echoed by the media and politicians. They caused the Basel EGS project to be stopped *sine die* after completion and stimulation of the first well. Induced seismicity is a fatal issue during the build up of any EGS reservoir, which happen to be hosted in seismically active tectonic environments. Therefore, accurate seismic monitoring/processing during all phases of a EGS project, along careful communication with the public are required to secure EGS, present and future, undertakings, a matter discussed by Rybach (2006).

## REFERENCES

- Antics, M.A. (1992). "Reservoir Simulation of the Tomnatic Geothermal Area. Romania", Geothermal Institute, University of Auckland, NZ, 59 pp.
- Antics, M.A. (1998). "Computer Modelling of an Over Pressured Medium Enthalpy Geothermal Reservoir Located in a Deep Sedimentary Basin". Proc., 23<sup>rd</sup> Workshop on Geothermal Reservoir Engineering, Stanford University, Stanford, California.
- Antics, M. (2004). "Low Enthalpy Reservoir Simulation". Proc. Int. Geoth. Days (IGD Poland), Zakopane, Poland, Sept. 2004.
- Antics, M., Papachristou, M., Ungemach, P. (2005). "Sustainable Heat Mining. A Reservoir Engineering Approach". Proc., Thirtieth Workshop on Geothermal Reservoir Engineering, Stanford University, Stanford, California, Jan. 31- Feb. 2, 2005.
- Aunzo, Z.P., Bjornsson G. and Bodvarsson, G.S. (1991). "Wellbore Models GWELL, GWNAFL and HOLA". Lawrence Berkeley National Laboratory Report LBL-31428, Berkeley, California, Oct. 1991.
- Aziz, K. (1997). "Fundamentals of Reservoir Simulation". Stanford University, Petroleum Reservoir Engineering Dept., Stanford, California, PE223, Winter 1997-1998.

- Bodvarsson, G. (1969). "On the Temperature of Water Flowing Through Fractures". *J. Geo. Res.*, **79**.
- Bodvarsson, G.S., Pruess, K. and O'Sullivan, M.J. (1985). "Injection and Energy Recovery in Fractured Geothermal Reservoirs", *Soc. Pet. Eng. Jour.*, **25**, n°2, 303-313.
- Bodvarsson, G.S. (1988). "Numerical Modelling of Geothermal Systems with Applications to Krafla, Iceland, and Olkaria, Kenya". Geothermal Reservoir Engineering, Okadan, E. (Edr). Kluwer Academic Press Publ., 297-316.
- Bourdet, D. (2002). "Well Test Analysis: The Use of Advanced Interpretation Models". Handbook of Petroleum Exploration and Production, 30, Elsevier.
- Butler, S.J., Sanyal, S.K., Robinson-Tait, A., Lovekin, J.W. and Benoit, D. (2001). "A Case History of Numerical Modelling of a Fault-Controlled Geothermal System at Beowave, Nevada". Proceedings, Twenty-Sixth Workshop in Geothermal Reservoir Engineering, Stanford University, Stanford, California, Jan. 2001.
- Castania, L., and Sanyal, S.K. (1980). "Geothermal Reservoir Modelling. A Review of Approaches", *Transactions, Geoth. Res. Comp.*, **4**, 313-316.
- Chierici, G.L. (1994). "Principles of Reservoir Engineering". Vol. 1, Springer Verlag Publ., Berlin.
- Clauser, C., Edr (2003). "Numerical Simulation of Reactive Flow in Hot Aquifers". SHEMAT and Processing SHEMAT. Springer Verlag Publ. Co., Berlin.
- Economides, M.J. and Miller, F.G. (1984). "Geothermal Reservoir Evaluation Considering Fluid Absorption and Composition", Paper SPE 12740, California Regional Meeting of the Society of Petroleum Engineers, 1984.
- Economides, M.J. (1987). "Physical and Thermodynamic Properties of Geothermal Systems". Applied Geothermics, Economides, M.J. and Ungemach, P. (Eds), John Wiley & Sons Ltd, 19-34.
- Economides, M.J. (1987). "Engineering Evaluation of Geothermal Reservoirs". Applied Geothermics, Economides, M.J. and Ungemach, P. (Eds), John Wiley & Sons Ltd, 91-110.
- Ehlig-Economides, C.A. and Economides, M.J. (1981). "Pressure and Temperature Dependant Properties of the Rock-Fluid Systems in Petroleum and Geothermal Formations, Paper SPE 9919, California Regional Meeting of the Society of Petroleum engineers, 1981.
- Fouillac, C., Sauty, J.P. and Vuataz, F.D. (1988). "Use of Tracers in the Geothermal Industry – Tracer Flow Equations in Porous Media", Geothermal Reservoir Engineering, Okadan, E. (Edr), Kluwer Academic Press Publ., 77-90.
- Garnish, J. (2002). "European Activities in Hot Dry Rock Research". US Dept. of En., Open Meeting on Enhanced Geothermal Systems, Reno, Nevada, Sept. 26-27, 2002, Summary Report.
- Gudmundsson, J.S. (1988). "Material Balance of Geothermal Reservoirs", Geothermal Reservoir Engineering, Okadan, E. (Edr), Kluwer Academic Press Publ., 143-156.
- Grant, M.A., James, R. and Bixley, P.A. (1982). "A Modified Gas Correction for the Lip Pressure Method". Eighth Workshop on Geothermal Reservoir Engineering, Stanford University, Stanford, California, Dec. 1982. SGP TR 60.
- Hadgu, T, Zimmermann, R.W. and Bodvarsson, G.S. (1995). "Coupled Reservoir-Wellbore Simulation of Geothermal Reservoir Behavior". *Geothermics*, **24**, 2, 145-166.
- Hallemburg, J.K. (1988). "Standard Methods of Geophysical Formation Evaluation". CRC Press LLC, Levis Publ., New York, NY.
- Havlena, D. and Odeh, A.S. (1963). "The Material Balance as an Equation of a Straight Line", *J. Pet. Tech.*, August, 896-900.
- Horne, R.N. (1988). "Geothermal Energy Assessments", Geothermal Reservoir Engineering, Okadan, E. (Edr), Kluwer Academic Publ., 7-21.
- Horne, R. (2002). "Modern Well Test Analysis. A Computer Aided Approach". 2<sup>nd</sup> Edition. Petroway inc., Palo Alto, California.
- Hsieh, C. (1980). "Vapor Pressure Lowering in Porous Media". Ph. D. Thesis,

- Stanford University. Stanford, California.
- James, R. (1962). "Steam-Water Critical Flow Through Pipes", Proc. Inst. Mech. Engrs., 176, 741.
- Keenan, J.S., Keyes, F.G., Hill, P.G. and Moore, J.G. (1969). "Steam Tables. Thermodynamic Properties of Water Including Vapors, Liquid and Solid Phases", John Wiley & Sons Ltd, New York.
- Kohl, T., Baujard, C. and Zimmermann, G. (2007). "Modelling of Geothermal Reservoirs, An Overview". ENGINE. Enhanced Geothermal Innovative Network for Europe, Mid Term Conference, Potsdam, Germany, January 9-12, 2007.
- Lasseter, T.J., Whitherspoon, P.A. and Lipman, M.J. (1976). "Multiphase Multidimensional Simulation of Geothermal Reservoirs". Proc. Second UN Symp. On Devel. and Use of Geothermal Resources, San Francisco, California, 3, 1715-1723.
- Lund, J.W. (2003). "The Use of Downhole Heat Exchangers". Geoheat Center. Oregon Institute of Technology, Klamath Falls, Oregon, USA.
- Matthews, C.S. and Russel, D.J. (1967). "Pressure Build Up and Flow Tests in Wells". Monograph, Vol. 1, Henry Doherty Series, Soc. of Pet. Eng. of AIME, New York, NY, Dallas, TX, USA.
- O'Sullivan, M.J. (1987). "Geothermal Reservoir Simulation", Applied Geothermics, Economides, M. and Ungemach, P. (Edrs), John Wiley & Sons Ltd, 111-124.
- O'Sullivan, M.J., Pruess, K., and Lippermann, M.J. (2001). "State of the Art of Geothermal Reservoir Simulation". *Geothermics*, 30, n°4, 395-429.
- Peaceman, D.W. and Rachford, H.H. Jr (1995). "The Numerical Solution of Parabolic and Elliptic Differential Equations". *J. Soc. Indust. Appl. Math.*, 3, 28-41.
- Pruess, K. Oldenburg, C. and Moridis, G. (1999). "TOUGH2 User's guide, Version 2.0", Lawrence Berkeley National Laboratory Report LBNL - 43134, Berkeley, CA.
- Pruess, K. (2002). "Mathematical Modelling of Fluid Flow and Heat Transfer in Geothermal Systems. An Introduction in Five Lectures", United Nations University Geothermal Training Programme, 2002, Report 3, Reykjavik, Iceland, Oct. 2002.
- Ramey, H.J. Jr and Nabor (1954). Unpublished Manuscript. Stanford University, Stanford, California.
- Ramey, H.J. Jr (1970). "A Reservoir Engineering Study of the Geysers Geothermal Field", submitted as evidence, Reich and Reich Petitioners vs. Commissioner of Internal Revenue, 1969 Tax Court of the United States, 52, T.C. No. 74.
- Ramey, H. Jr (1988). "Transient Pressure Testing in Geothermal Systems". Geothermal Reservoir Engineering (Okandan, E. Edr). Kluwer Academic Publishers, 55-62.
- Rose, P.E., Apperson, K.D., Johnson, S.D. and Adams, M.C. (1997). "Numerical Simulation of a Tracer Test at Dixie Valley Nevada", Proc., 22<sup>nd</sup> Workshop On Geothermal Reservoir Engineering, Stanford University, Stanford, California.
- Rose, P.E., Johnson S.D. Kilbourn, P. and Kasteler, C. (2002). "Tracer Testing at Dixie Valley, Nevada, Using 1 - Naphtalene Sulfonate and 2.6 - Naphtalene Disulfonate". Proc., 26<sup>th</sup> Workshop on Geothermal Reservoir Engineering, Stanford University, Stanford, California, January 28-30, 2002.
- Rybach, L., Mégel, T. and Engsten, W.J. (1999). "How Renewable Are Geothermal Resources". *Trans. Geoth. Res. Council*, 23, Oct., 17-20, 1999.
- Rybach, L. (2003). "Geothermal Sustainability and the Environment". *Geothermics*, 32, 463-470.
- Rybach, L. (2007). "Induced Seismicity During EGS Operation". ENGINE. Enhanced Geothermal Innovative Network for Europe. Simulation of Reservoir and Induced Seismicity, Workshop 3, Zürich, 29 June - 01 July, 2006.
- Sanyal, S.K. (2005). "Geothermal Resource: Characteristics, Development and Ma-

- nagement". World Geothermal Congress (WGC 2005), Izmir/Antalya, Turkey, April 2005. Pre and Post Congress Short Courses, Popovski, K. (Edr), Di Pippo, R., Sanner, B. and Ungemach, P. (convenors), 261-347.
- Sanyal, S.K. (2005). "Sustainability and Renewability of Geothermal Power Capacity", Proceedings, World Geothermal Congress 2005, Antalya, Turkey, April 24-29, 2005.
- Schlumberger (1986). "Log Interpretation Charts". Schlumberger Well Services.
- Schlumberger (1987). "Log Interpretation Principles/Applications". Schlumberger Educational Services.
- Ungemach, P. (1987). "Electric Power Generator from Geothermal Sources". Applied Geothermics (Economides M.J. and Ungemach, P. Edrs). John Wiley & Sons Ltd, 137-187.
- Ungemach, P., Ventre, A.V. and Nicolaon, S. (2002). "Tracer Leak Off Tests as Means of Checking Well Integrity. Application to Paris Basin Geothermal Production Wells". Proc., 27<sup>th</sup> Workshop on Geothermal Reservoir Engineering, Stanford University, Stanford, California, Jan. 28-30, 2002.
- Ungemach, P. (2003). "Reinjection of Cool Geothermal Brines into Sandstone Reservoirs". *Geothermics* **32**, 743-761.
- Ungemach, P., Antics, M. and Papachristou, M. (2005). "Sustainable Geothermal Reservoir Management". Proc. World Geothermal Congress (WGC 2005), Antalya, Turkey, 24-29 April, 2005.
- Ungemach, P., Papachristou, M., Antics, M. (2007). "Renewability vs. Sustainability. A Reservoir Management Approach", Proceedings, European Geothermal Energy Congress, 2007, Unterhaching, Germany, 30 May – 1 June, 2007.
- Varga, R.S. (2000). "Matrix Iterative Analysis, 2<sup>nd</sup> Ed.", Springer Series in Computational Mathematics, Springer Verlag Publ. Co., Berlin.
- Warren, J.E. and Root, P.J. (1963). "The Behaviour of Naturally Fractured Reservoirs". *SPE. J.*, September, 245-255. Whiting, R.L. and Ramey, H.J. Jr (1969). "Applications of Material and Energy Balances to Geothermal Steam Production", *J. Pet. Tech.*, July, 893-900.

